(4) (5) 2 790

(1) BSD-TDR-62-348 (3) RESEARCH REPORT 143

(6) STAGNATION POINT HEAT TRANSFER MEASUREMENTS IN PARTIALLY IONIZED AIR

(7) by

P. H. Rose and J. O. Stankevics

AVCO-EVERETT RESEARCH LABORATORY
a division of
AVCO CORPORATION
Everett, Massachusetts

(11) Contract No. AF 04(694)-33

(12) April 1963

prepared for

HEADQUARTERS
BALLISTIC SYSTEMS DIVISION
AIR FORCE SYSTEMS COMMAND
UNITED STATES AIR FORCE
Air Force Unit Post Office
Los Angeles 45, California

(1) NA
(3) NA
(4) NA
(12) 49 p
(15) NA
(16) NA
(17) NA
(20) U
(21) NA

ABSTRACT

Experimental measurements of convective stagnation point heat transfer in partially ionized air at simulated flight velocities up to 55,000 ft/sec are presented, ~~in this paper~~.

Stagnation point heat transfer rates were measured in an arc-driven shock tube. The operation of this tube was carefully monitored by a variety of diagnostic techniques, mostly using emitted radiation as the observable. Although the performance of an arc-driven shock tube has been found to be quite predictable, it is shown that proper auxiliary measurements must be made for each experiment to identify those regions where proper flow conditions exist.

Calorimetric heat transfer gages, either coated with silicon-monoxide films or uncoated, were used to measure heat transfer. The effects of boundary layer chemistry, ~~radiation from the hot inviscid flow~~, and instrumentation errors are discussed. Comparison is made of the measured heat transfer rates with other data and the points of agreement and disagreement are analyzed.

The data are compared to theoretical predictions made with a simple binary diffusion model of partially ionized diatomic gas, ~~namely,~~ nitrogen, whose transport properties were estimated from measured and calculated cross-section data. Stagnation point heat transfer rates calculated from this model for both a frozen and an equilibrium boundary layer, as well as equilibrium boundary layer results from other available calculations using more elaborate models of air, are compared to the data. The applicability of frozen and equilibrum calculations are discussed.

Although it is not possible to differentiate between a number of the very similar theoretical treatments of this problem from the present results, it is concluded that the transport properties of air up to 15,000° K are known to reasonable accuracy and that heat conduction by electrons does not present a serious engineering problem for flight velocities up to 50,000 ft/sec.

Introduction

The possibility that the great mobility of electrons in highly ionized gases could have the effect of enhancing heat conduction in a boundary layer in such a gas has been an area of considerable speculation and some research over recent years.[1]-[3] The lack of conclusive experimental data and the difficulties of calculating and measuring the transport properties of such gases have left this question in a state of uncertainty. Recently, the stagnation point heat transfer in partially ionized air has been the center of considerable controversy. At present there are serious uncertainties in both the available theoretical and experimental results.

The experimental investigation of the stagnation point heat transfer in partially ionized air reported herein was initiated to help answer the questions raised by various theoretical and experimental treatments.[4]-[9] In order to achieve this purpose we felt that a minimum requirement of the scope of the present experiments should be threefold, i.e.,

(1) A thorough scrutiny of the operation of the shock tube and verification of the existence of a homogeneous hot gas sample.

(2) Extension of the velocity range of the experiments to conditions where a dominant fraction of the energy is invested in ionization.

(3) Collection of a sufficient quantity of data to allow for meaningful statistical analysis.

Experimentally, the problem of heat transfer in ionized air differs from the lower speed, dissociated air situation in two respects, each presenting major difficulties. The first is the problem of creating ionized air of known or calibrated composition in which the measurements are to be made. The second problem arises because the diagnostic techniques which have been developed for heat transfer measurements have their difficulties when applied to highly conducting gases. The first of these two problems was solved by the development of the electric arc-driven shock tube.[8][10] Arc-driven shock tubes capable of producing equilibrium degrees of ionization in air as large as 60% have been operated successfully. The other problem has been overcome by improvements in the experimental techniques involved with heat transfer gages. In this paper we will discuss, first, the shock tube and the verification of the gas conditions under which the heat transfer measurements were made, secondly, the heat transfer instrumentation and special techniques which were required to validate the results of this investigation, and, finally, the experimental heat transfer results and their import in the light of our present knowledge of the heat transfer mechanism, transport properties, and associated phenomena.

Shock Tube

The experiments were performed in an electric arc-driven shock tube, 6 inches in diameter and approximately 30 feet long.[10] In this device a strong shock wave is created by the discharge of up to 90,000 joules of electric energy into a light gas confined in the driver section. The discharge creates a longitudinal arc column along the axis of the driver between the electrode and the diaphragm region in which the gas is heated by joule dissipation to a very high temperature. The column expands and the conditions equalize throughout the driver gas, helium in the present experiments, and temperatures of approximately 20,000° K are achieved. As the arc energy is transferred to the gas, the driver pressure rises to a maximum value. A diaphragm separating the driver from the driven, or test, section bursts at approximately this instant and a strong shock wave propagates down the shock tube.

In an ideal operation this shock wave heats, compresses and accelerates the test gas and continually accumulates test gas between the shock and the expanding driver gas. However, in a violent process, such as is needed to create the extreme temperature and pressure conditions demanded by this experiment, the shock tube processes are far from ideal. In such a situation the question of the proper definition of the actual test gas conditions must be carefully scrutinized.

The operation and performance of this type of shock tube were discussed in detail in reference (10). The non-ideal aspects of the operation start in the driver section. Here, the intense radiation from the arc column, and later from the 20,000°K driver gas, creates large losses and causes evaporation of the driver walls. These effects result in shock strengths considerably less than those predictable from an ideal theory. However, it is common practice to measure the actual shock velocity in each experiment so that this non-ideal aspect of the shock tube operation does not affect the experimental data. However, these phenomena do limit the highest velocities achievable in this type of shock tube. More important to the present experiments are the finite time required by the diaphragm to open and the probable asymmetries in the diaphragm opening process. Asymmetries in the energy distribution in the driver could also occur. All of these effects introduce disturbances into the driver gas at its interface with the test gas which may grow as the interface proceeds down the shock tube. For high velocity operation, the interface may be unstable because a dense gas is pushing a less dense one while the whole system is decelerating. This Taylor-type of instability helps the turbulence at the interface to grow. Lastly, the boundary layer acts as a path by which the gas in the test slug can escape through the interface.[11] This effect is best seen by considering the mass flow past the interface in an interface-fixed coordinate system. In this frame of reference, the gas immediately adjacent to the wall flows out of the test slug past the interface into the driver gas region at a velocity equal to the velocity of the wall relative to the interface, which is equal to the negative of the flow velocity behind the shock, i.e., $-U_2$.

The performance of the shock tube has been carefully evaluated under the conditions of the present experiments. The efficiency of energy transfer, i.e., from the condenser storage to the form of kinetic energy imparted to the test slug, was disucssed in reference (10). Figure 1 shows the electrical energy which must be delivered to the driver to produce a given shock velocity.

Measurement of the shock velocity alone is not enough to verify the proper operation of a high performance shock tube. The test time must be carefully observed and monitored for its duration, steadiness, and other characteristics. The test time loss due to the flow of gas past the interface in the boundary layers has been calculated for the present experiments from the theory of Roshko,[11] using boundary layer calculations for a variable fluid properties model as suggested in reference (10). The calculated values of test time duration are compared to the measured performance in Fig. 2. The measured data were obtained by observing the radiation from a one-dimensional thin slab of the test gas with a photomultiplier having approximately one-half microsecond time resolution. The test time was judged as the distance between the onset of radiation in the form of the non-equilibrium overshoot and the increase in radiation when the interface arrives. Samples of the observed radiation profiles are shown in a later section. Although only a fraction of the calculated test time is actually achieved, the observed radiation profile duplicates the ideal picture, i.e., a non-equilibrium overshoot followed by a steady equilibrium region which is terminated by a sudden rise of intensity at the first indication of the arrival of the interface. The enhanced radiation at the interface must be explained as evidence of the presence of driver gas and/or wall or diaphragm impurities in a region which is still predominantly hot test gas. This region lasts approximately 50μ sec and its intensity varies directly with the peak driver temperature, i.e., the amount of foreign material in the driver gas. The later driver region in which the driver gas dominates the temperature is, of course, quite cold.

The present performance of electric arc-driven shock tubes has allowed simulation of stagnation conditions of flight velocities as high as 56,000 ft/sec. The principle of stagnation point simulation in shock tubes and the Mach number independence of stagnation point heat transfer experiments were discussed in detail in reference (12). Figure 3 shows the shock tube operating conditions superimposed on a flight velocity-altitude grid at those points where identical stagnation conditions are produced in the two situations. The present operating range and limits of the 6-inch arc-driven shock tube are also shown. Typical reentry trajectories for vehicles with an L/D of 0.5 are also included in the figure. It can be seen that the low density limit of a 6-inch shock tube (at high shock velocities) of about 100μ initial pressure misses density simulation of the trajectories by about 1 order of magnitude.

Instrumentation

Shock tube heat transfer measurements have been performed mainly by two techniques*; namely, the thin film resistance thermometer[13] and the thick resistance thermometer or calorimeter.[14] The relative merits of the thin and calorimeter gages were discussed in references (12) and (13). For the present application, the choice was clear. Where high heat transfer rates are involved, thin gages require that large corrections be made to account for the non-uniform thermal properties of the resistance element and the back-up material as the surface temperature rises significantly.[16] The low resistance of the calorimeter gages make them simpler to insulate from the gas in cases where such insulation is necessary to electrically separate the currents in the gage from the ionized, conducting gas. For these reasons, calorimeter gages were used exclusively in the present experiments.

Another advantage of the calorimeter gage is the ability to dispense with gage calibration. In reference (14), the properties of chemically pure platinum were checked by dynamic calibrations, and it was concluded that the static bulk material properties were usable in data reduction. This procedure has again been followed in the present experiments.

Heat transfer gages were mounted at the stagnation point of hemispherical noses of cylindrical models of 0.635 and 1.27 cm radius. The techniques described in references (12) and (14) were used. Several views of a typical calorimeter gage mounted on a model are shown in Fig. 4. The gage elements were either mounted directly on the model surface or were recessed to a depth of their own thickness without any noticeable difference in results.

The results which have been achieved with the calorimeter gages have been gratifying. During the initial experiments erratic pick-up was observed at the instant the shock passed the gage. These erratic signals often lasted through much of the test time. By careful shielding and proper balancing of the gage and oscilloscope circuit, it was possible to eliminate almost all spurious signals (except the first few microseconds) and to produce repeatable results. This result was observed both when the gages were covered by a thin coating of either silicon-monoxide or silicon-dioxide, approximately 0.1 microns thick. No significant qualitative differences in the data or their absolute value could be detected between coated and uncoated gages except at the highest shock velocities experienced. Only at shock velocities of 10 mm/μsec and above, insulating coatings were found to be necessary for obtaining easily interpretable data. A number of typical oscillograph records from heat transfer gages are shown in Fig. 5. Data are shown throughout the velocity range of the experiment. The data at the lower

* Recently, an infrared heat transfer gage has been developed which holds great promise for this type of measurement in highly conducting gases.[15]

velocities are generally of better quality. Equivalent data were obtained by both coated and uncoated gages up to the highest shock speeds.

Several theoretically predictable gage effects can be clearly identified in the data. The time required to establish an equilibrium flow geometry about the model, as discussed in reference (17), is shown in Fig. 6. This time was longer for 1.27 cm nose radius models than for the 0.635 cm ones, on the average approximately 4 and 3 microseconds, respectively. Several 5 cm diameter models were run to obtain data over a larger range of this variable. There was a general trend of shorter transient times for stronger shocks, i.e., the transient became shorter as the sound speed at the stagnation conditions increased. However, the data were too scattered to allow quantitative analysis of this effect.

When thinner gage elements were used, heat loss through the rear face of the element to the model was noticeable. This effect was evidenced by a curvature of the normally linear slope of the calorimeter records. As predicted,[14] platinum gage elements .0007 and .0008 inch thick readily showed this effect. Following the analysis of that reference, this effect could be corrected in data reduction. Figure 7 shows data obtained with .0007 and .0013-inch thick gages. The correction for heat loss to the backing brings the non-linear data from the thinner gage element close to linear, while the thicker element is not affected by the correction. If the gage element is made too thick, the heat does not penetrate the gage in the test time and the temperature distribution in the gage becomes highly non-linear.[12] The analysis of calorimeter data assumes a linear temperature distribution in the gage element. A second order correction term can be written for this effect. Rather than utilizing this correction, the situation has been avoided by use of sufficiently thin gage elements.

One other observation was made which, however, remains unexplained. In an effort to check the work reported by Warren,[8] gages .003 and .004 inch thick, as used by Warren, were used. These gages showed a reproducible but unexplained curvature of the signal output through much of the test time. In these gages reproducible signals of the same order as the desired data were produced, even when no current was passed through the gage, i.e., when no resistance thermometer effect could possibly be measurable. The thinner gages used in the present experiments always produced the desired negative (no signal) result when the gage circuit was intentionally left open during a run. Data from .003 and .004-inch thick platinum gage elements were consequently not considered usable in this series of experiments.

The reproducibility of the data presented is not as good as one might hope for from this type of data. The largest error appears to be introduced by gage uncertainties, particularly the difficulty of knowing the precise value of the resistance corresponding to the effective gage area and the contact resistance of the connections to the gage

element. Measured gage resistances of approximately plus or minus 15 percent of the value computed from the handbook resistance and the assumed effective gage dimensions were common. The difficulty is one of obtaining a voltage change measurement which is entirely due only to the resistance element which is sensitive to the heat pulse. If the gage resistance measurement includes any resistance other than that of the effective gage element undergoing the resistance change due to the calorimeter effect, this difference will appear to be an increment in heat transfer in the data. The data collected from certain gages showed considerably more scatter than the data from other gages. However, no a priori reasons for this occurrence have been established. In general, only two to five runs were made with a given gage and, consequently, no selection rules have been found for good gages.

All other measurements were made with far greater accuracy. Initial pressures and shock velocity were measured with better than 3 percent accuracy. The pressure was measured by an alphatron and McCloud gage and the velocity by the output from a number of upstream side-wall heat transfer detectors. The output was displayed on a raster presentation on a standard oscilloscope for ease of reading small time intervals accurately. Immediately in front of the model the shock velocity was measured again by three photomultipliers, this time to better than 2 percent accuracy. In data reduction the shock velocity was extrapolated to the gage location. The output of the heat transfer gages was recorded on Tektronix 535 oscilloscopes with differential preamplifiers, 53/54D. A Ballentine voltage standard was recorded on the oscillogram for every experiment. It must thus be assumed that the conditions of the flow were known accurately in every experiment and that the measurements were taken with sufficient accuracy to produce data with a maximum deviation of less than 10 percent. The balance of the scatter of the data must be attributed to the gage uncertainties.

Auxiliary Measurements

Heat transfer measurements have been obtained at initial shock tube pressures of 1 mm and 0.25 mm and shock velocities of 6 to 12 mm/μsec. For each experiment auxiliary measurements were made to verify the proper operation of the shock tube while the heat transfer measurement was being made. This appears like an extreme measure compared to standard shock tube techniques, but it has been our experience that the operation of shock tubes under these extreme conditions is occasionally erratic and such verification is essential to prevent misleading results.

The standard auxiliary measurements made for every experiment were radiation profiles of microsecond time resolution taken with photomultipliers viewing across the shock tube. Time resolution of about one-half microsecond was obtained through the use of collimated narrow slits. Proper operation of the shock tube was judged by the appearance of a non-equilibrium overshoot of the proper width and intensity,[18] followed by an approximately steady radiation level indicative of the

equilibrium region in the test gas. The test is considered terminated when the first evidence of the interface is seen. In arc-driven shock tubes this is usually a sudden rise of radiation intensity when the driver gases or driver impurities first appear. A selection of typical radiation histories is shown in Fig. 8.

Two other measurements have been made, however, on a more sporadic basis. These were image converter pictures which visualize the whole test gas due to its luminosity, and observations of the radiation from the inviscid flow field behind the bow shock in the stagnation region. The image converter gives a vivid view of the state of the test gases. The non-equilibrium shock front, steady equilibrium region and interface are clearly visible. The interface is seen to be a region of large scale, non-axial motion, i.e., turbulence, even in experiments where a test time is clearly visible. In such experiments the test time correlates with, but is always less than, the test time predicted in reference (10). Turbulent mixing between the driver and driven gas at the interface probably accounts for this departure from the theory. The violence of this turbulence determines what fraction of the calculated test time is actually achieved. There is no apparent systematic difference between experiments which show a finite test time and ones in which the interface turbulence is sufficient to consume all the test gas. It can be shown from elementary considerations that if the characteristic mean turbulent velocity is larger than $U_2\rho_1/\rho_2$, i.e., the flow velocity behind the shock, U_2, multiplied by the density ratio across the shock, ρ_1/ρ_2, then the turbulent interface will grow sufficiently to consume all the test gas. For the case of strong shocks in air, this requirement means turbulence levels of less than 5 percent. Examples of image converter data, together with corresponding photomultiplier records, are shown in Fig. 9 for two experiments, one in which a finite test time is visible and one where there is no test time.

The other measurements involved looking at the radiation emanating from the inviscid flow region between the bow shock and the body at the stagnation point. A photomultiplier was directed to view a point in the flow one-half millimeter in front of the stagnation point through a set of vertical collimated slits approximately one-half millimeter wide. For a 1.27 cm radius model, the standoff distance of the shock at the stagnation point is approximately 2 mm. A careful examination of the oscillograph records from this measurement shows a number of phenomena which verify the proper operation of the shock tube. When the incident shock passes the field of view of the slit, a small but very steep rise can be seen. The shock reflected from the model comes into view after a fraction of a microsecond and the radiation intensity rises by about an order of magnitude. The initial fast rise becomes more gradual in this region, lasting about 5 μsec. We attribute this to the time required for the bow shock geometry in the field of view of the photomultiplier to reach its final configuration. This should require slightly more time than the boundary layer transient shown in Fig. 6. Following the rise, an approximately steady radiation intensity is seen until the interface arrives. These characteristics are visible in the

sample oscillograms shown in Fig. 10.

One other measurement was made in a number of experiments. A time-resolving drum camera spectrograph with f 4 optics was set up to view the inviscid flow in front of the stagnation point. Although no high quality spectra have been taken tc date, it was clearly evident in the data taken that no non-air sources of radiation were visible during the 15 to 20 μsec test time. The air-nitrogen band structure[19] was identifiable.

The described auxiliary data give a clear knowledge of the test time limitation for each experiment. This aspect of the performance of arc-driven shock tubes has also been documented thoroughly in reference (10). A two and one-half foot long constant-diameter section has been added to the shock tube immediately downstream of the diaphragm. It was hoped that this section would give the shock a better chance to form and separate from the interface before entering the expansion section where the diameter changes from one and one-half to six inches. The result of this modification has been a slight loss in shock velocity, about 1 mm/μsec, but a clear increase in the average test time and also an increase in the number of runs showing a homogeneous hot gas sample. Typical test time data, as observed from the radiation profiles behind the incident shock front both before and after the modification, were shown in Figs. 2a and 2b. The data from experiments performed after the installation of the constant diameter section showed less randomness, and lay along the upper edge of the data band.

State of Test Gas

Having established proper operation of the shock tube and the existence of a homogeneous gas sample under the experimental conditions, it still remains to determine the thermochemical state of the test gas. In making this determination, the three regions involved, i.e., the gas behind the incident shock, the stagnation region, and the boundary layer, must be considered. All three regions must be considered both from the point of view of the dissociation and the ionization mechanisms.

The state of the dissociation processes can be established from the extensive available literature of the chemical kinetics of air.[20] Behind strong normal shock waves, the distance or time required by a flow to relax to a thermodynamic equilibrium state can be calculated from the rates summarized by Wray.[20] The observations of Allen, et al[18] of the time required for the radiation from the molecular bands of nitrogen to return to the equilibrium level after the initial overshoot at the shock front are a measure of this equilibration time (or distance) and can be applied to the present experiments. Figure 11 shows these results calculated for the conditions of this experiment by the application of binary scaling.[18] The corresponding data observed from the photomultiplier viewing across the shock tube, discussed in the previous section, are also shown. The measurements generally agree with the interpretation of Allen's data except at the high shock velocities

where the non-equilibrium region was not resolved. It can be concluded that at initial shock tube pressures of 0.25 mm and higher, and test times of 6 μsec and more, almost all of the incident gas is in dissociation equilibrium, except possibly at the lowest shock velocities used.

The relaxation process in the gas behind the standing or bow shock wave in front of the model is another aspect of the same question. Due to the much higher temperatures, the relaxation is considerably faster, but the characteristic length, in this case the shock detachment distance, is also much smaller than the length of homogenous gas sample available. The time or distance required for the dissociation process to equilibrate in this gas can be estimated by extrapolating the same data[18]. In order to apply these data we calculated the moving normal shock which creates conditions identical to the experimental stagnation conditions. For this calculated incident normal shock, the dissociation relaxation time or distance can be converted into a particle time. This particle time was then assumed to apply to the flow behind the bow shock in the inviscid region. The resulting distances required by the air to equilibrate behind the standing or bow shock are shown in Fig. 12. Also shown are the shock detachment distances for two model sizes used in this experiment. The equilibration distances are seen to be equal to, or smaller than, the stand-off distance over most of the experimental range. Only the low shock velocity, 0.25 mm initial pressure experiments can be in some doubt. The estimate made above is felt to be conservative because the definition of equilibrium as the point where radiation intensity has relaxed to only 10 percent above the equilibrium level[18] is very conservative in the present context of determining the departure from equilibrium. Also, in a two-shock process, i.e., where half the enthalpy is added across the incident shock and half across the bow shock, equilibration across the bow shock is probably faster because of the elevated energy level of the incident gases. However, the data of reference (18) were extrapolated by about 50 percent in velocity. From the above consideration it is felt that the dissociation process is in equilibrium at the edge of the boundary layer throughout the present experiments.

The final consideration of the equilibration of the dissociation process concerns the state of the gas throughout the boundary layer, i.e., does the chemistry remain in equilibrium or does it freeze at some point as it is quenched by the wall? The conditions under which a boundary layer will be completely in equilibrium, completely frozen, and in some intermediate state, were determined by Fay and Riddell's numerical solutions for a reacting stagnation point boundary layer.[21] In this reference a parameter, C_1, is proposed to measure the state of recombination in the boundary layer, as follows:

$$C_1 = K_1 \left(\frac{P_s}{R} \right)^2 T_s^{-3.5} \left(\frac{dUe}{dx} \right)^{-1}$$

where $K_1 T^{-1.5}$ was derived from the oxygen recombination rate and its temperature dependence,[22] P_s is the stagnation pressure, T_s is the stagnation temperature, R is the universal gas constant, and dUe/dx is the velocity gradient at the stagnation point. This parameter is essentially the ratio of the oxygen three-body recombination time to the flow time of a particle in the boundary layer. It was shown that when this parameter reaches a value of one, the boundary layer starts to freeze. However, a value of 10^{-4} is required before the freezing is sufficient to affect the heat transfer strongly, i.e., a recombination parameter of less than 10^{-4} is required before the effects of the degree to which a surface can catalyze atom recombination, i.e., the catalytic efficiency, can be seen in the heat transfer measurement. Thus, equilibrium boundary calculations should be valid for $C_1 > 1.0$, frozen boundary layer calculations for $C_1 < 1.0$. However, for surface effects to be a possible source of differing heat transfer measurements, a value of $C_1 < 10^{-4}$ is required. The above results were shown to be valid for a wide range of flow conditions and surface temperatures by Goodwin and Chung.[23]

In evaluating this parameter, the room temperature recombination coefficient for oxygen atoms was taken to be 1.0×10^{15} $cm^6/mole^2$-sec from a recent review of the available data.[24] It is now known that the actual temperature dependence of the oxygen recombination process is much weaker, in fact $T^{-1/2}$ or even non-existent.[25] This lesser temperature dependence will change the calculation of the point of onset of boundary layer freezing. The form of the recombination coefficient suggested by Goodwin and Chung[23] has allowed Inger[26] to propose a correlation which accounts both for variations of the temperature dependence of the recombination rate coefficient and the wall or surface temperature. Combining this correction with C_1 from reference (21), we get

$$C_1 = K_1 T^{\omega} \left(\frac{P_s}{RT_s}\right)^2 \left(\frac{dUe}{dx}\right)^{-1}$$

and

$$C_1^* = C_1 \left(\frac{Tw}{300}\right)^{\omega-2}$$

where ω is the temperature dependence exponent discussed above. The recombination parameter calculated from the above equation is shown in Fig. 13. The velocity dependence is very weak and a single line suffices for the range of this experiment. The value of the coefficient, C_1^*, was below unity for all the present experiments but was not low enough so that surface effects could be measurable.

Much less evidence is available to ascertain the state of the ionization process. Shock tube measurements of the ionization rate for air have been made by Lin and Fyfe[27] at shock velocities up to 7 mm/μsec.

The experimental results are in agreement with the complex system of reactions and rates proposed by Lin and Teare.[28] The conclusion from this work was that the atom-atom reactions completely dominated the ionization process in the experiments, and the calculations show this condition to exist up to shock velocities of 9 mm/μsec. At this shock velocity, i.e., temperature, it is expected that the electron impact process will become fast enough to dominate the ionization rate, and extrapolations of the data of Lin would not be meaningful. There is also some question about the impact ionization mechanism stipulated by Lin. Lin considers direct, one-step ionization from the ground state only. However, ionization can proceed via the upper levels and such a process can be considerably faster. Thus electron impact may become important at even lower shock velocities than calculated in reference (28). Keeping these uncertainties in mind, the ionization distances behind the incident shock calculated from the mechanism proposed by Lin are shown in Fig. 14. The times required are all considerably less than the test time and appear to decrease with increasing shock speeds. It is also noteworthy to observe that the ionization process is always faster than the dissociation chemistry in the regions where data are available.

The uncertainty about the ionization state behind stronger incident shocks is due to our present lack of knowledge of the dominant process in this region. However, the atom-atom process is already very fast at 9 mm/μsec and a process would have to be even faster to dominate the overall ionization rate. This argument leads to some assurance that ionization equilibrium should exist behind the incident shock. In opposition to this argument is the fact that the strongest shock calculation made for the Lin model considers equilibrium ionization of only fractions of one percent, whereas at the fastest shock velocities about 20 percent ionization exists behind the incident shock if the air is in equilibrium. Consequently, ionization must proceed at considerably faster rates for the process to be complete in the same time, distance or number of collisions. The above argument admits the possibility that the total ionization distance may become longer at higher shock velocities. The state of ionization behind strong incident shocks is thus uncertain at this time.

The state of ionization in the inviscid flow, i.e., the conditions at the edge of the boundary layer, suffers from the same uncertainties. It can only be stated that no experimental conditions have ever been observed in which ionization was not equilibrated when the dissociation chemistry reaches completion. Thus, it can be hoped that this chronology of equilibration is again upheld and ionization equilibrium precedes the dissociation whose relaxation times were shown in Fig. 13.

The last equilibration question to be treated is the question of electron recombination in the boundary layer. Assuming complete thermodynamic equilibrium at the edge of the boundary layer, we can again resort to interpreting and extrapolating the work of Lin.[28] Most electrons are removed from a hot gas by the inverse of the atom-atom collision processes, i.e.,

$$N + N \rightleftharpoons N_2^+ + e$$

$$N + O \rightleftharpoons NO^+ + e$$

where the above two reactions were shown to dominate the total electron production in air. At high temperatures, a competing path is offered by the inverse of the electron impact process, i.e., electron-electron-ion three-body recombination.

$$N + e \rightleftharpoons N^+ + e + e$$

The experiments of reference (27) give a basis for estimating the maximum rate of removal of electrons at outer edge of the boundary layer for the first of these processes. Lin's data were shown to be reasonably explainable by a recombination coefficient for both of the N_2^+ and NO^+ processes of

$$k_R \cong 3 \times 10^{-3} \; T^{-3/2}$$

The time rate of change of number of electrons for the two-body recombination processes can be written as

$$\frac{d[e]}{dt} = \left(k_F [N]^2 - k_R [N_2^+] [e] \right) + \left(k_F [N] [O] - k_R [NO^+] [e] \right)$$

where k_F and k_R are the forward and reverse rate coefficients, respectively. The maximum rate of change of number of electrons for a displacement from equilibrium occurs when the forward reactions are zero, and as the recombination coefficients for the two processes are equal, can be written as

$$\left(\frac{d[e]}{dt} \right)_{max} = -k_R [e][N_2^+ + NO^+]$$

Substituting the recombination coefficient given above, gives

$$\frac{d \ell n [e]}{dt} = -3 \times 10^{-3} \; T^{-3/2} [N_2^+ + NO^+]$$

and the characteristic time required for the electron concentration to deplete by a factor of e is

$$\Delta t = \frac{T^{3/2}}{3 \times 10^{-3} [N_2^+ + NO^+]} = \tau_{1\,ion}$$

The characteristic flow time can be defined as $\left(\frac{dUe}{dx}\right)^{-1}$ which is the time required by a particle to flow a distance equal to the nose radius, and thus also the time for a particle to diffuse through the boundary layer at the stagnation point. In a Newtonian flow,

$$\left(\frac{dUe}{dx}\right)^{-1} \cong R\sqrt{\frac{\rho_s}{2(P_s)}} = \tau_{flow}$$

The ratio of the above two flow times is plotted in Fig. 15 for the experimental stagnation conditions. Note that because the equilibrium concentration of N_2^+ and NO^+ becomes very small for strong shocks, electron recombination becomes very slow due to this mechanism. In fact, if this were the only mechanism for removal of electrons, the electron recombination in the boundary layer would freeze at high shock velocities.

As stated previously, the electron three-body recombination process will compete with the previous reactions for removal of electrons at high temperatures. For this reaction we can write

$$\frac{d[e]}{dt} = k_F [N] [e] - k_R [N^+] [e]^2$$

At equilibrium the forward and backward rates are exactly equal, and consequently we can use either to estimate the maximum possible depletion rate. Using the forward process, we get

$$\frac{d\,\ell n\,[e]}{dt} = [N]\ k_F$$

In studying the forward process in a shock front, Lin argued that ionization should proceed from the ground state and that ionization from the excited upper levels need not be considered. On this basis, by estimating the collision cross section he arrived at the following rate for the forward process,

$$k_F \cong 0.55 \times 10^{-10} \; e^{-169,000/T} \sqrt{T}$$

Consequently,

$$\frac{d[n[e]}{dt} = [N] \; 0.55 \times 10^{-10} \; e^{-169,000/T} \sqrt{T}$$

and the characteristic time for this process can be written as

$$\Delta t = \frac{1.82 \times 10^{10}}{[N]} \quad \frac{1}{e^{-169,000/T} \sqrt{T}} = \tau_{2 \text{ ion}}$$

The ratio of this time to the flow time has been calculated as shown in Fig. 15. It can be seen that the combination of this result and the atomic reactions allow the possibility of a region of experimental conditions in which the electron recombination process freezes at the edge of the boundary layer.

For a recombination process starting from a high temperature equilibrium state, it is more likely that the populated upper excited levels will accelerate mechanism by allowing transition between closely spaced levels to become recombinations by subsequent cascading to the ground state. This mechanism was considered by Bates.[29] The so-called collisional-radiative recombination coefficient for hydrogen is tabulated in this reference. It is further stated that the collisional radiative decay is not very sensitive to the species of simply charged atoms. Using the tabulated values, ~~a third~~ ion relaxation time, $\tau_{3 \text{ ion}}$, can be calculated. This time is much shorter than $\tau_{2 \text{ ion}}$ and would take over as the dominant recombination mechanism at sufficiently low shock velocities so that electronic equilibrium will be maintained in the boundary layer throughout the range of the present experiments.

The conclusion which has been tentatively drawn from these considerations of the electronic equilibration is that in all likelihood the flow will equilibrate in the boundary layer but its state at the boundary layer edge is not known precisely in the present experimental series. From a relative argument with respect to the dissociation process, it is speculated that equilibrium does exist. The state of knowledge of the ionization mechanism at high temperatures is not sufficient at this time to allow any such statements to be made with great confidence.

Heat Transfer Results

The heat transfer data deduced from the present series of experiments are shown in Fig. 16. The heat transfer rates have been normalized by the square root of the nose radius to combine the data from various gage sizes. Only data points from experiments during which at least 6 microseconds of test time were clearly verified by one of the methods described have been used. This restriction has separated out the apparent scatter which would be introduced by analyzing data before the initial transient had subsided (see Fig. 6). Data were taken at two initial shock tube pressures, 1.0 and 0.25 mm of Hg of air, simulating flight at altitudes of approximately 110,000 and 140,000 ft, respectively. The shock velocity range accessible in the arc-driven shock tube has been covered, reaching a simulated velocity of 55,000 ft/sec at the lower initial pressure, i.e., 0.25 mm. Models with spherical noses at 0.635 and 1.27 cm radius were used.

Heat transfer gages with and without thin silicon monoxide coatings were used in the experiments. In many cases the uncoated gages were the same physical gages, only on a second run after the coating had been eroded away during the initial experiment. Gages were polished between experiments to remove any residue of the coatings for second or uncoated experiment. Although silicon monoxide and platinum have vastly different catalytic efficiency [30] for atom recombination, no difference in heat transfer is to be expected if the inviscid flow was in thermodynamic equilibrium or if the boundary layer chemistry was not sufficiently frozen, as discussed in the previous section. The average values of the data from coated and uncoated gages taken separately varied by only several percent.

The data are compared with the results calculated by the Fay and Kemp binary diffusion model for ionized diatomic gases. [31] Both equilibrium and frozen boundary layer calculations for nitrogen as the working fluid are shown for comparison with the data. The transport properties of nitrogen were expressed as simple functions of temperature and concentrations, as discussed in references (31) and (32). The data appear to follow the theoretical predictions in a general way.

A curve fit has been made to all the data after they were further normalized by dividing the heat transfer rate times the square root of the nose radius, $q\sqrt{R}$, by the square root of the stagnation pressure, $\sqrt{p_s}$. The theoretical dependence of this parameter on stagnation pressure, i.e., simulated altitude or density, is weak as evidenced by the effect of varying the stagnation pressure over a factor of 100 in the calculation of the heat transfer parameter, Nusselts divided by square root Reynolds no., $Nu/\sqrt{Re}$. [31] The stagnation pressure varied from about one to 30 atmospheres in these experiments. The data and quartic curve fit (dotted line) are shown in Fig. 17. The root mean square deviation of the data from this curve is 0.13. The solid line was calculated from the correlation equations of Reference 31 for the equilibrium boundary layer for a Lewis number of 0.6 for the experimental

conditions of 0.25 mm initial pressure. At an initial pressure of 1 mm of Hg, the theory would be 8 percent higher at 10 mm/μsec.

The most striking aspect of the comparison between the experiments and theory is the disagreement in the intermediate velocity range. The mean of the experimental points lies approximately 20 percent below the theories in the 7 to 8 mm/μsec velocity range. A number of effects have been considered to explain this discrepancy.

The possibility that the gas at the edge of the boundary layer was not in equilibrium and that this would in turn affect the heat transfer was investigated. Calculations were performed for cases in which the gas was not allowed to ionize, i.e., ionization was frozen. The ionization energy was redistributed and thus resulted in a much greater temperature. However, as has been experienced in other heat transfer problems in the past, the heat transfer rates were found to be essentially independent of the division of the energy among the various modes and dependent mainly on the total energy. Consequently, lack of ionization equilibration is not felt to be a cause for the difference.

Another suggestion which has been made is that the discrepancy is due to the difference between nitrogen and air. It has been suggested by Fenster and Rozycki[45] that this difference is indeed due to differences between nitrogen and air. In support of their argument, they point to several effects which could contribute to the phenomena in question. First, reference 45 points out that Fenster and Heyman[46] have found that the diffusion of energy at the wall is dominated by the oxygen dissociation energy which is only about half the value of the nitrogen dissociation energy. Inclusion of this distinction in a theoretical calculation has resulted in heat transfer rates in dissociated air approximately 30 percent less than calculated from Fay and Riddell. However, Kemp has pointed out that the additional terms considered by Fenster and Heyman to account for the oxygen dissociation energy are only a partial inclusion of the effects due to the diatomic nature of air, and other effects probably of equal significance as those considered, were discounted. This result must be considered as inconclusive at this time.

To treat the ionized air case, Fenster and Rozycki used the transport properties of Peng and Pindroh.[47] Comparing the total conductivity of reference 47 with those of Yos[39] and those of Hansen,[38] significant differences are seen to exist, although the assumptions, cross sections and methods used vary too much to identify the source of the differences.

Yos[39] has, however, calculated the transport properties of air and nitrogen by the same method. The result of his calculations are reproduced in Fig. 18. Although the differences between air and nitrogen in general are small, there are some significant differences. Of course, the total conductivity of air is somewhat larger (a factor of two)

in 3000 to 4000°K due to the recombination energy of NO. However, at about 7000 - 8000°K, nitrogen has a higher equilibrium or total conductivity by about 30 percent. It should be noted that this region is almost exactly where the heat transfer rates measured in air are significantly lower than the nitrogen theory. The air thermal conductivity of Yos[39] and Peng and Pindroh[47] agree very well in this temperature range. At higher temperatures the differences between nitrogen and air are negligible according to Yos.* Thus at very high speeds one would expect the nitrogen theory to be a better approximation for air than it was at lower speeds. The latter effect can be seen in the data.

In order to further validate the use of a nitrogen theory for air, a number of experiments were performed in nitrogen. These data are shown in Fig. 17 as crosses. As expected, the agreement of the mean of these data with the air values in the high shock velocity range was quite satisfactory. However, in the 7-8 mm/μsec shock velocity range, where the air conductivity according to Yos is lower, the nitrogen and air data also agreed with each other. Thus, the measured nitrogen heat transfer rates were also some 20 percent less than predicted by the theory. Arguments based on the differences between air and nitrogen must consider these data. The use of the binary diffusion nitrogen model as a basis for comparison of theory and air experiments appears justified but all questions are still not completely settled.

The possibility of the Lewis number being lower than the assumed value was also considered. The theory for a frozen boundary layer with Lewis number approximately 0.3[31] appears to follow the experimental data quite reasonably. However, it has not been possible to devise a reasonable argument why the boundary layer should be frozen or why the Lewis number should have such a small value.

Finally, the applicability of any boundary layer theory in which all constituents have the same temperature must be questioned. At present no boundary layer theories which allow variations of the electron temperatures exist. This question appears to be a fruitful area of future research.

The large differences between the heat transfer from the equilibrium and frozen boundary layer calculations at high shock velocites are a striking result of Reference (31) which emphasizes the importance of knowing the precise thermodynamic state of the gases at the edge of the boundary layer. In the dissociated boundary layer case, the total heat transfer could only be affected by extreme freezing, $C_l < 10^{-4}$, in combination with noncatalysity of the surface. In the ionized case, no surface effects were needed to alter the heat transfer. Thus, the above difference is a new phenomena and should be understood.

---

* Ref. 47 calculates the conductivity of air to be considerably greater than the nitrogen values calculated by Yos.

The difference in heat transfer results between the two boundary layer calculations apparently is a result of the binary diffusion model. Because the charge exchange cross sections for collisions between like particles, i.e.,

$$N^+ + N \rightleftharpoons N + N^+$$

are apparently almost an order of magnitude greater than the kinetic cross sections, the atoms and ions essentially lose their identity and cannot diffuse relative to each other. The electrons are tied to the ions to diffuse together by charge neutrality (ambipolar diffusion). Thus, as far as diffusion is concerned, there are really only two components in an ionized diatomic gas, atom, ion and electron combinations and molecules.

In the equilibrium boundary layer the ion concentration drops very sharply quite close to the outer edge. The atom concentration peaks in the middle of the boundary layer and the molecule concentration starts to build up deep in the boundary layer as the atom concentration starts to decrease.[31] The result of combining these concentrations with the binary diffusion model is that as there are no molecules in the boundary layer in places where there are ions, and thus there is no diffusion between ions and molecules; consequently, no ionization energy can diffuse to the wall. In fact, there appears to be no diffusion at all in the outer part of the boundary layer. In the frozen boundary layer, the ion concentration does not decrease sharply and some ionization persists through the boundary layer. Consequently, ions and molecules coexist in this boundary layer and diffusion of ionization energy to the wall can proceed.

The experimental data appear to bear out the validity of such a model. The experiments were performed under assumed equilibrium or near equilibrium conditions and the measured heat transfer is depressed below the frozen calculations.

A further consideration of the experimental results was an estimate of the magnitude of the contribution to the measured heat transfer which could be attributed to radiative heating. Radiation data for air at the temperature, density and degree of ionization which are encountered in this experiment are not very complete. The various existing radiation calculations and tables[33]-[35] are either based on data obtained at lower temperatures or are purely theoretical calculations. Their results differ by a factor of two at the experimental conditions of this study. An analysis of the differences between these tables has been made by Keck.[36] He concluded that calculations based on emission measurements are preferable to those derived from theoretical calculations of high temperature emission from discharge or absorption measurements at room temperature. The only emission data obtained under the proper conditions are the preliminary measurements reported

in reference (37). As these data have not yet found their way into a complete radiation calculation, the work of Kivel[33] has been utilized in this study for estimating radiation. These calculations agree within a factor of two with the other available tables.[34][35]

The ratio of the equilibrium radiative heating to convective heating rates calculated from the data discussed above for complete absorption by the gage surface is shown in Fig. 19. The largest value of this ratio encountered under the conditions of this experiment was 0.3 at the maximum velocity and dropped very rapidly with shock velocity. In view of the fact that the gage material certainly does not absorb all of the incident radiation, and that the results of reference (37) appear to indicate that the radiation predicted by Kivel may be high by a factor of about 2 in this temperature region, no effort was made to apply this result as a correction.

One other source of radiation was considered but discarded. It has been noted that the driver gas radiates quite intensely (see Fig. 8). This radiation is incident on the gage even before the shock arrives at the gage and the aerodynamic heating occurs. The strength of the source of this radiation varies only slowly as the shock wave proceeds down the shock tube, and the solid angle subtended at the gage by this source of radiation changes. During the interval between the time when the incident shock is one tube diameter upstream of the gage and the time the interface arrives to this point, the solid angle viewed changes by a factor of about 3. Thus, if this source produced significant heating at any time during the experiment, it should also be visible before the arrival of the incident shock front. No such signal has ever been detected by heat transfer gages.

Comparison with Other Theories and Experiments

Figure 20 shows a summary of the theories and data on heat transfer in partially ionized air and nitrogen known to the authors. The stagnation point heat transfer rates calculated from the theories of Hoshizaki,[4] Pallone,[6] Cohen,[7] and Fay and Kemp,[31] agree within plus or minus 25 percent up to velocities of 55,000 ft/second. Note that the calculations of Hoshizaki, Cohen, and Pallone for air all used the transport properties of Hansen[38] and are essentially equivalent analyses. The difference between their results must thus be attributed to numerical differences, and the particular correlation equations proposed by the authors for their numerical results. The differences between these results are a good measure of the accuracy which may be expected from this type of boundary layer calculation.

Pallone[6] has used the transport property calculations of Yos[39] for his calculations for nitrogen. These calculations may be compared directly with the work of Scala.[5] Scala's calculation is for a four-component mixture of nitrogen, i.e., atoms, molecules, ions and electrons. The transport properties of this mixture were calculated as part of the program, as discussed in reference (40). It was suggested [41]

that the high heat transfer rates calculated by Scala were due to the small charge exchange cross section for the diffusion of nitrogen ions through nitrogen atoms utilized in this theory. This cross section, as used by Scala, was over 2 orders of magnitude smaller than the corresponding value calculated by Yos, following the method of Mason.[42] The latter is very close to comparable cross sections measured in rare gases.[32]

Pallone has proven the above premise to be correct.[6] He has used both the cross sections of Yos[39] and Scala[40] in calculations for nitrogen. A difference of more than a factor of 2 in the heat transfer rates above 35,000 ft/sec, and a difference of 2 orders of magnitude in the thermal conductivity resulted. Using the experimental thermal conductivity measurements in nitrogen obtained by Maeker[43] from arc experiments, Pallone shows close agreement with the heat transfer rates calculated using the transport properties of Yos.[39]

It must be concluded from the data and discussion presented here that the predictions of Scala[5][40] vary from other theories due to his choice of a charge exchange cross section which is considerably smaller than that calculated by Yos. Although the heat transfer data presented in this paper are not capable of differentiating between the various theories, i.e., Pallone, Cohen, Hoshizaki, and Fay and Kemp, they certainly confirm the applicability of all of these theories as opposed to that of Scala. Consequently, the data are also an implicit verification of the transport properties of Hansen or Yos used in these calculations. At high temperatures the data of Yos appears preferable. It is also interesting to note that the simple binary diffusion model used by Fay and Kemp predicts that data trend as well as the more complex theories, and thus there is a strong indication that the binary diffusion model is valid for the ionized air case.

It is not as easy to identify the origin of the differences existing between the various experimental results shown in Fig. 20. There are now four sets of experimental data available which bear on this question. The present data are the most extensive and their validity can be judged from the earlier sections of this paper. The data of Offenhartz, et al[9] were obtained under conditions where test time is questionable, or at best very short,[10] i.e., approximately 5 microseconds. Hoshizaki[4] has presented data which verify his and the other similar theories. Although the data are not extensively documented in this reference, it is reasonable to assume from the conditions under which the experiments were performed that the data are valid.

Only the data of Warren[8] disagree with these three independent sets of data. Warren's data were obtained in an arc-driven shock tube in which the experimental test time was claimed to be precisely the value calculated for this shock tube in Reference (10). It has been our experience that all measured shock tube test times are considerably shorter than those calculated from the theory of Roshko.[11] Even

the data reported by Roshko, as well as the recent data of Hacker, et al,[44] which appear to agree with the calculated test time give experimental test times considerably shorter than the calculated value when corrected by using the boundary layer calculations of Reference (10). As seen in Fig. 2, a value of one-half the calculated time can be considered to be an upper bound. This is physically reasonable because the theory accounts only for the mass flow through the interface via the boundary layer; it ignores boundary layer effects on the shock front, and the finite opening time of the diaphragm, and turbulence and mixing at the interface. All these effects reduce the test time below the calculated value. It is consequently improbable that the Roshko test time can be achieved.

Warren's measurements were made with relatively thick calorimeter heat transfer gages, some of which were made of platinum and some of a nickel alloy steel called HYTEMCO. In the present experiments anomalous effects were observed with platinum gages of the thickness used by Warren. Correlation of this result with the data of Warren was not possible, however. On the basis of the data presented, the high heat transfer results of Warren must be considered to be anomalous, as the data from the three other independent investigations overwhelmingly support the lower levels predicted by the theories of Pallone, Hoshizaki, Cohen, and Fay and Kemp.

Summary

This experimental study has tried to deal with the difficulties which are encountered when shock tubes are operated in the high enthalpy range for the purpose of making heat transfer measurements. We have presented our data in some detail to emphasize the difficulties and the limitations that are imposed on our ability to accumulate meaningful data. Although some questions have been left unanswered, the data which have been presented are proven to be valid and techniques for making this determination are outlined.

The significance of the data is clear. The high heat transfer rates predicted by Scala are not borne out by the data, and it must be concluded that the high thermal conductivity which he calculated was erroneous. The data do agree with, but cannot differentiate between, the theories of Fay and Kemp, Pallone, Cohen and Hoshizaki, although they do favor the lower estimates at the high velocities. However, the differences between various calculations utilizing the same transport properties are of the same order as is the difference between the mean of the data and any one of the theories. It must also be concluded that there are no major unknowns in the transport properties of high temperature air up to 15,000°K and degrees of ionization of 50 percent. The largest uncertainties remaining in the interpretation of these data involve the definition of the exact state of the gases as well as a better understanding of the transport properties of nitrogen and air and their differences.

Acknowledgment

The authors would like to acknowledge many fruitful discussions with Dr. Nelson Kemp and Prof. James Fay, and the able assistance of Mr. Charles Saunders, Jr., in the operation of the experimental equipment.

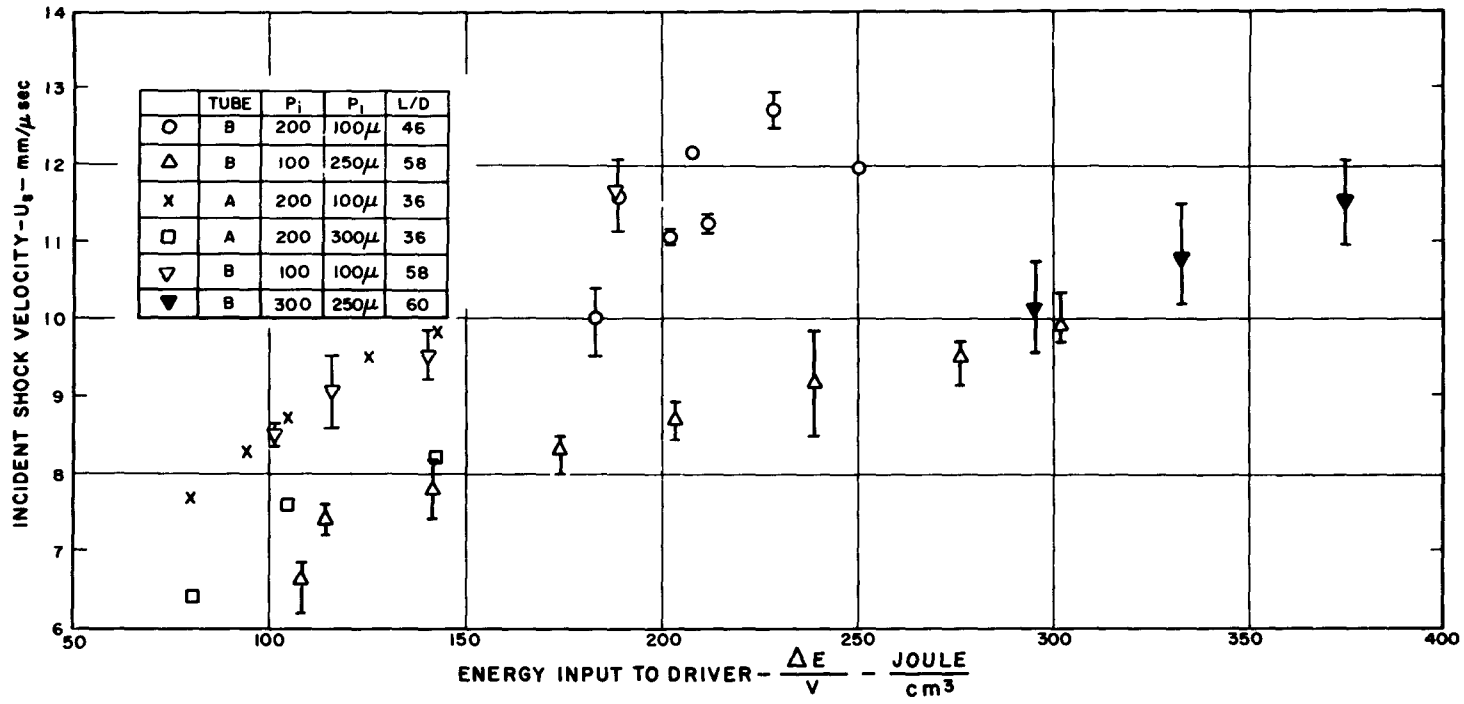

Fig. 1 Shock velocities measured in arc-driven shock tubes. The scatter bars on points indicate the average and variation among a large number of experiments performed at a given driver condition.

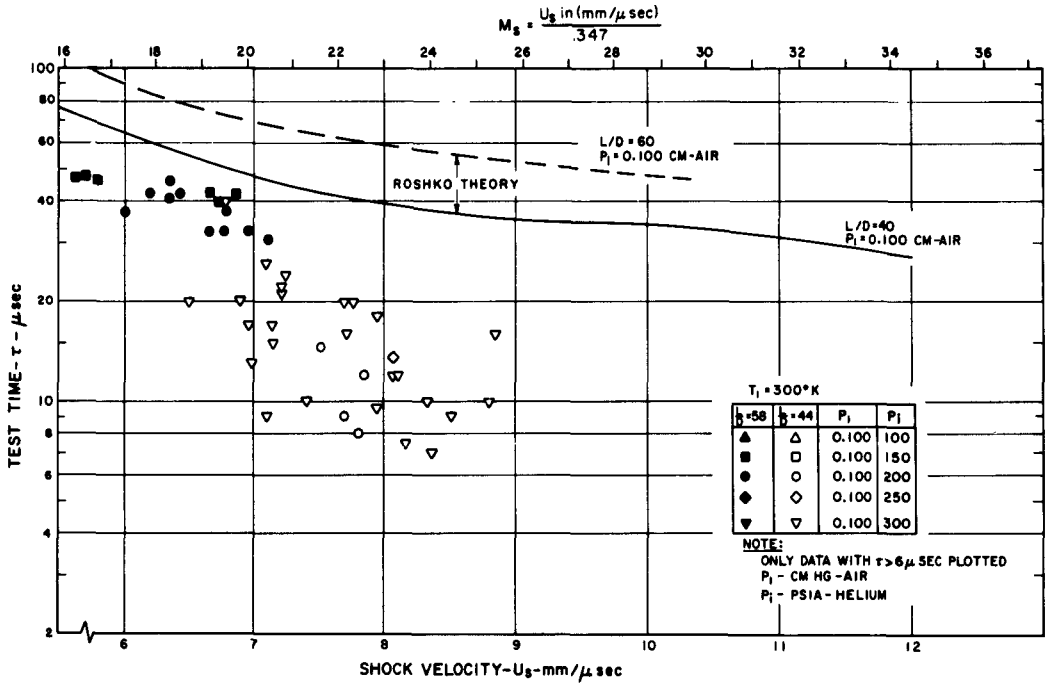

Fig. 2 (a) Time interval between the arrival of the shock front and the first indication of the arrival of the interface as measured from radiation emission. The data are compared to the calculated test time based on the Roshko[11] theory, modified by the boundary layer corrections of Ref. (10).

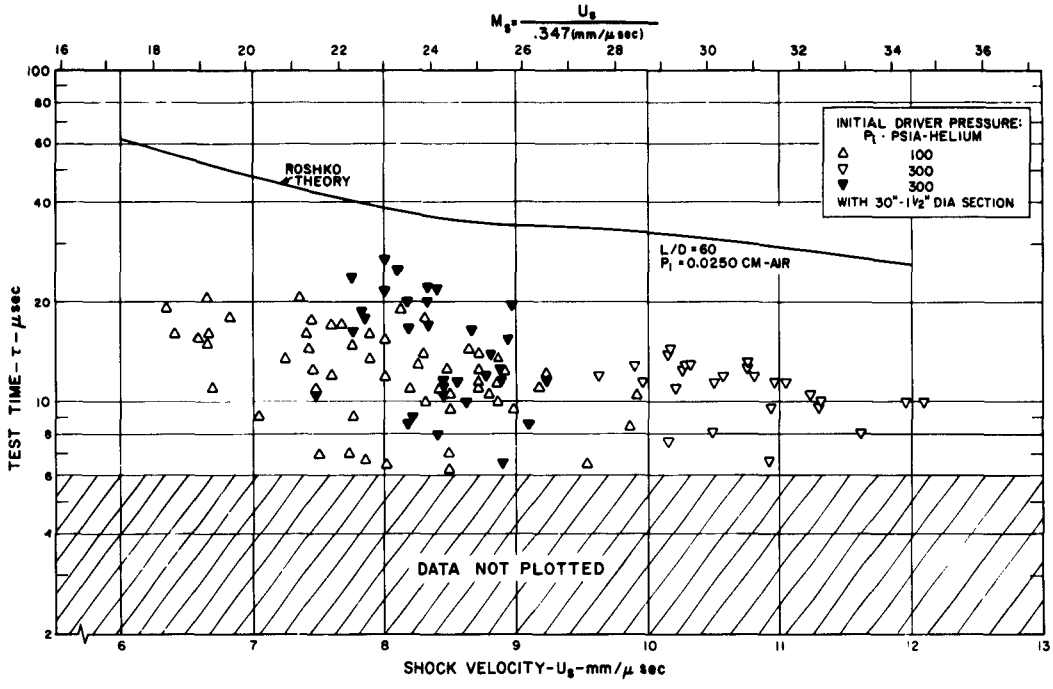

Fig. 2(b) Time interval between the arrival of the shock front and the first indication of the arrival of the interface as measured from radiation emission. The data are compared to the calculated test time based on the Roshko[11] theory, modified by the boundary layer corrections of Ref. (10).

Note the improvement of the average test time measured after the installation of the 30 ft long, 1-1/2 in. dia. section immediately downstream of the diaphragm.

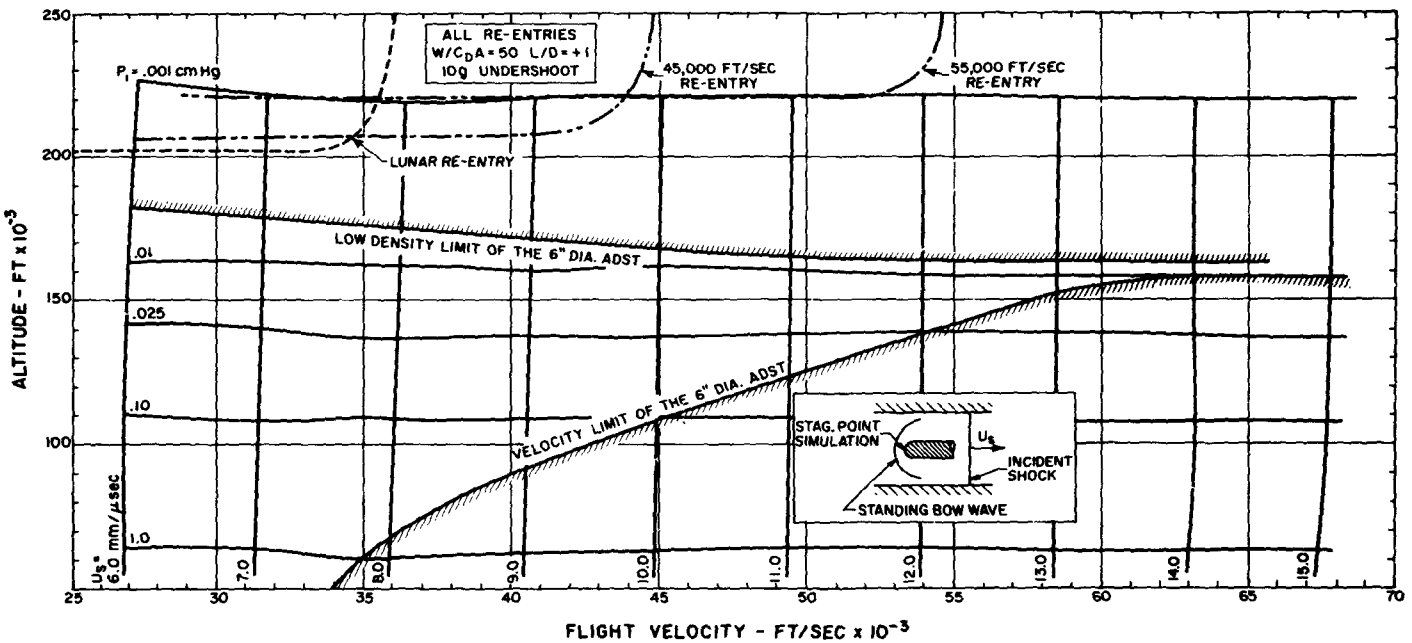

Fig. 3 Stagnation point simulation[12] in a high velocity shock tube. The shock tube conditions, i.e., shock velocity and initial pressure, are plotted on an altitude flight velocity grid at the points where identical stagnation conditions are achieved. The maximum deceleration trajectories of typical lifting re-entry vehicles (L/D ~ 0.5) for various entry velocities are shown for reference.

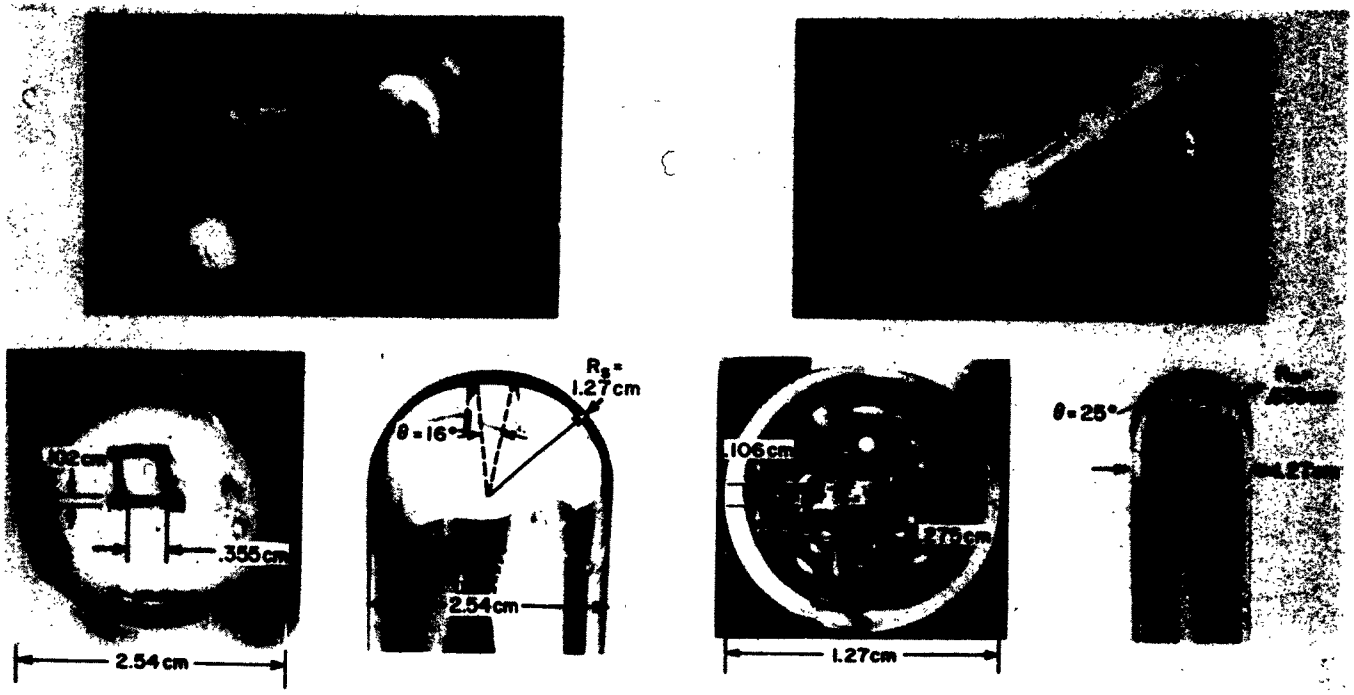

Fig. 4 Typical calorimeter heat transfer gages mounted at the stagnation point of 0.635 and 1.27 cm nose radii hemisphere-cylinder glass models.

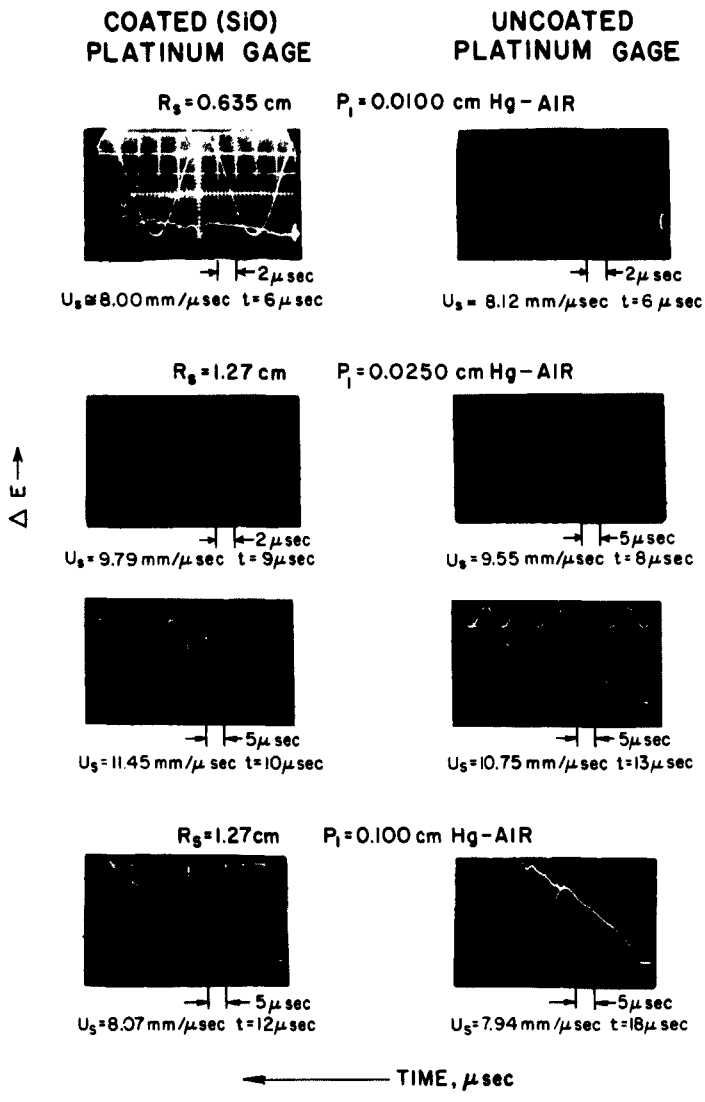

Fig. 5 Oscillograms of heat transfer records taken with uncoated and coated (Si O) calorimeter gages. After the initial transient, the gage output rises approximately linearly with time characteristic of a steady heat transfer rate. Data from various shock velocity experiments are shown. Data from the slower shocks are generally of better quality and show longer test time. Maximum and minimum slopes of each oscillogram were measured to estimate the uncertainty of the measured rates. The accuracy of each experiment was considerably better than the run to run repeatability.

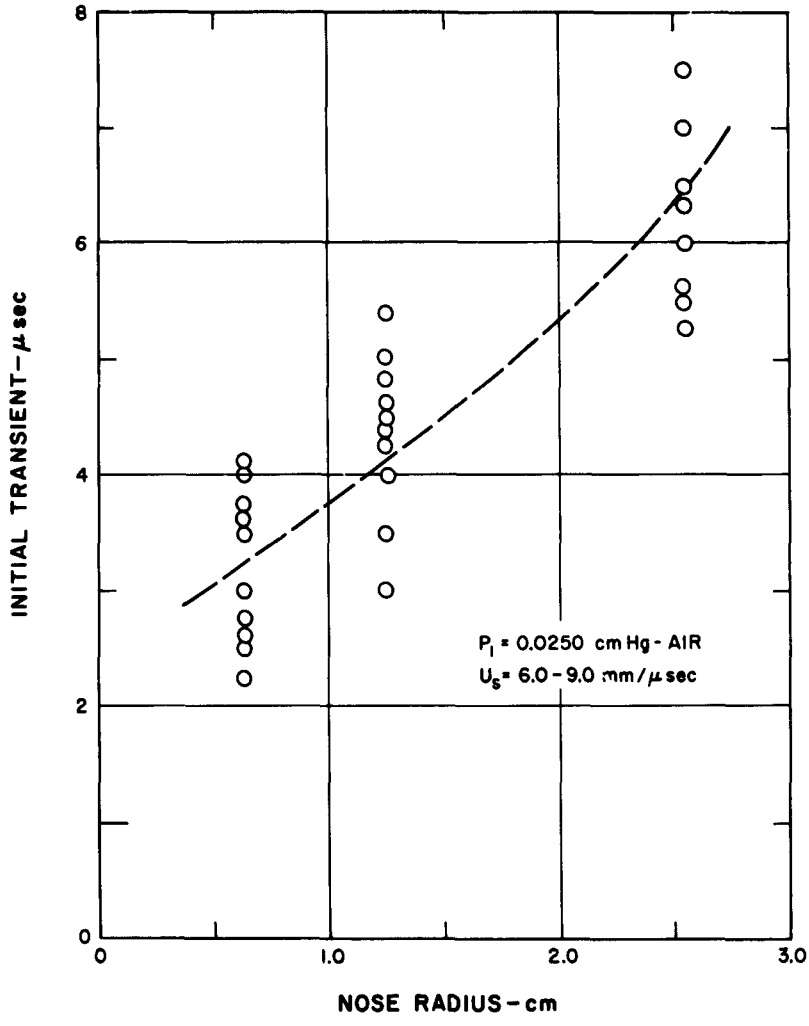

Fig. 6 Time required to establish steady flow about the heat transfer models. The time duration of the initial electrical transient is shorter than the time at which the initial curvature of the oscillogram terminated. This point is assumed to indicate the time at which the boundary layer and the shock curvature (i.e., stagnation point velocity gradient) achieve a steady geometrical configuration.[17]

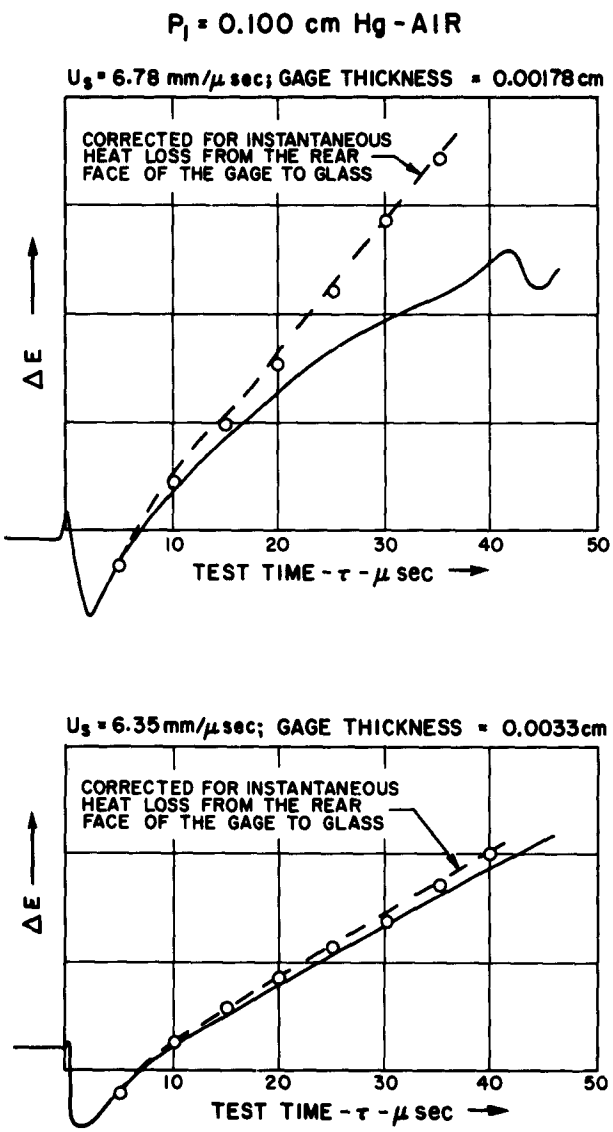

Fig. 7 Correction of heat transfer gage output for the heat loss through the rear surface of the gage.[12] Corrections are shown for a gage which is too thin and one which is of the proper thickness for the experimental conditions.

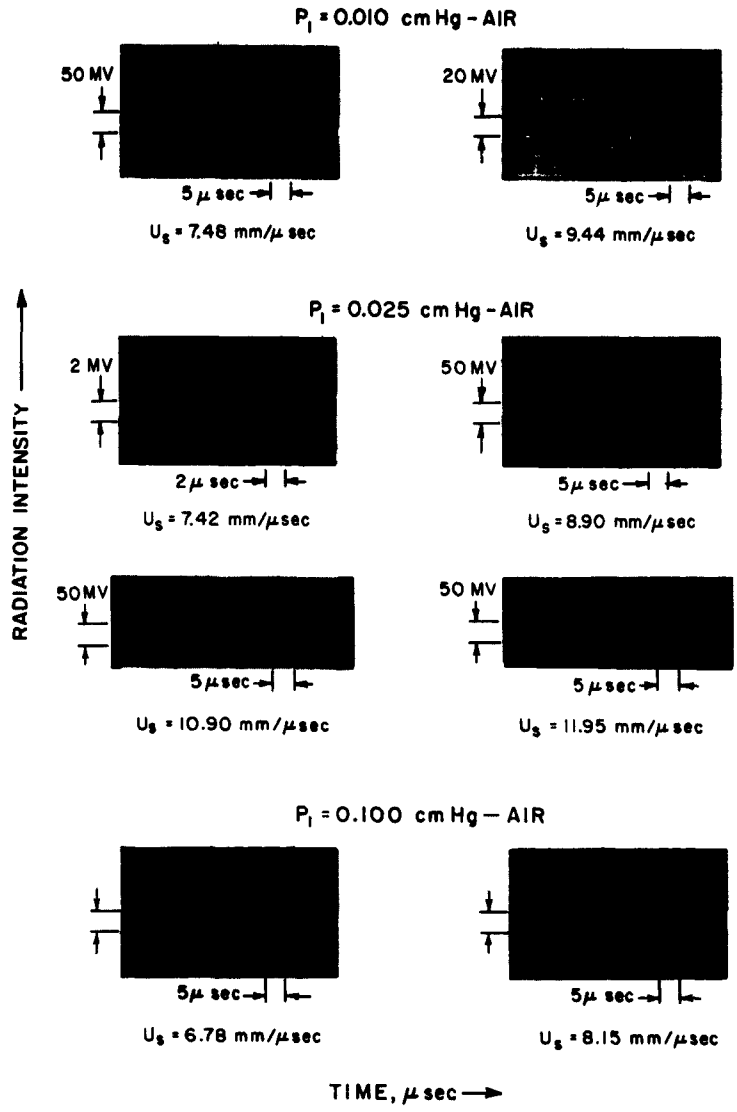

Fig. 8 Profiles of visible radiation emission in the 0.4 to 0.6μ wavelength region. The radiation profiles were recorded by a photomultiplier viewing through a set of collimated slits across the shock tube. Profiles show the radiation history behind the incident shock, i.e., the non-equilibrium region, the steady equilibrium zone, and finally strong emission from the interface. Intense interface radiation is typical of arc-driven shock tubes and can be adjusted by altering the driver conditions. This excess radiation lasts for approximately 50μ secs.

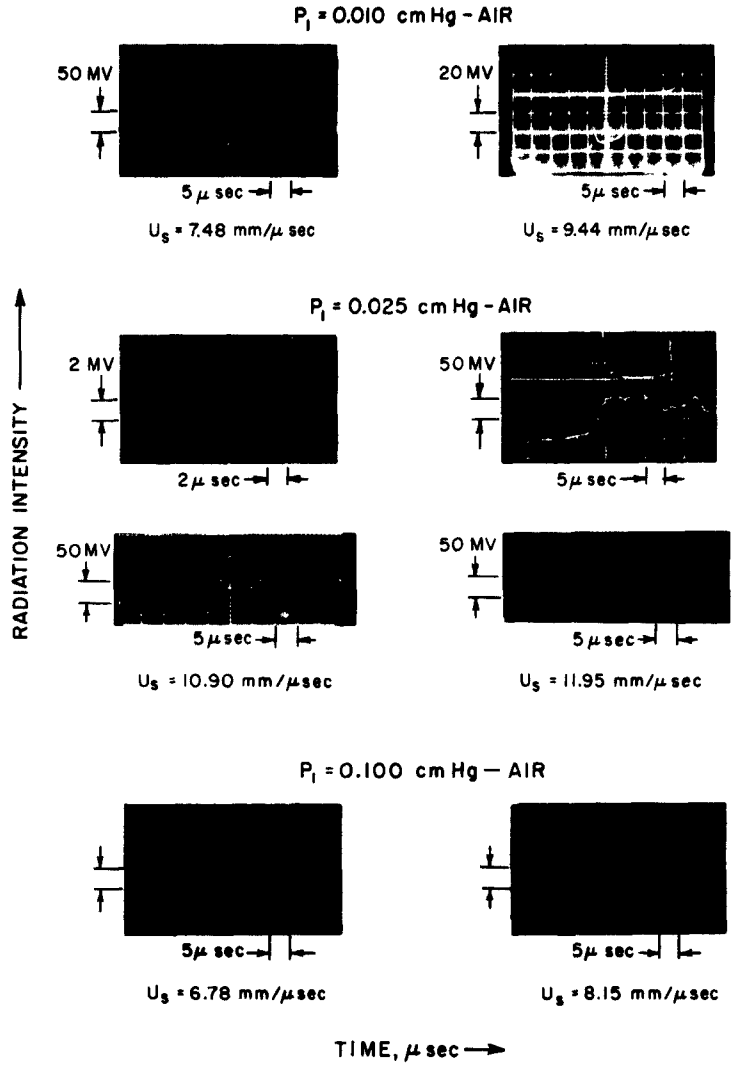

Fig. 8 Profiles of visible radiation emission in the 0.4 to 0.6μ wavelength region. The radiation profiles were recorded by a photomultiplier viewing through a set of collimated slits across the shock tube. Profiles show the radiation history behind the incident shock, i.e., the non-equilibrium region, the steady equilibrium zone, and finally strong emission from the interface. Intense interface radiation is typical of arc-driven shock tubes and can be adjusted by altering the driver conditions. This excess radiation lasts for approximately 50μ secs.

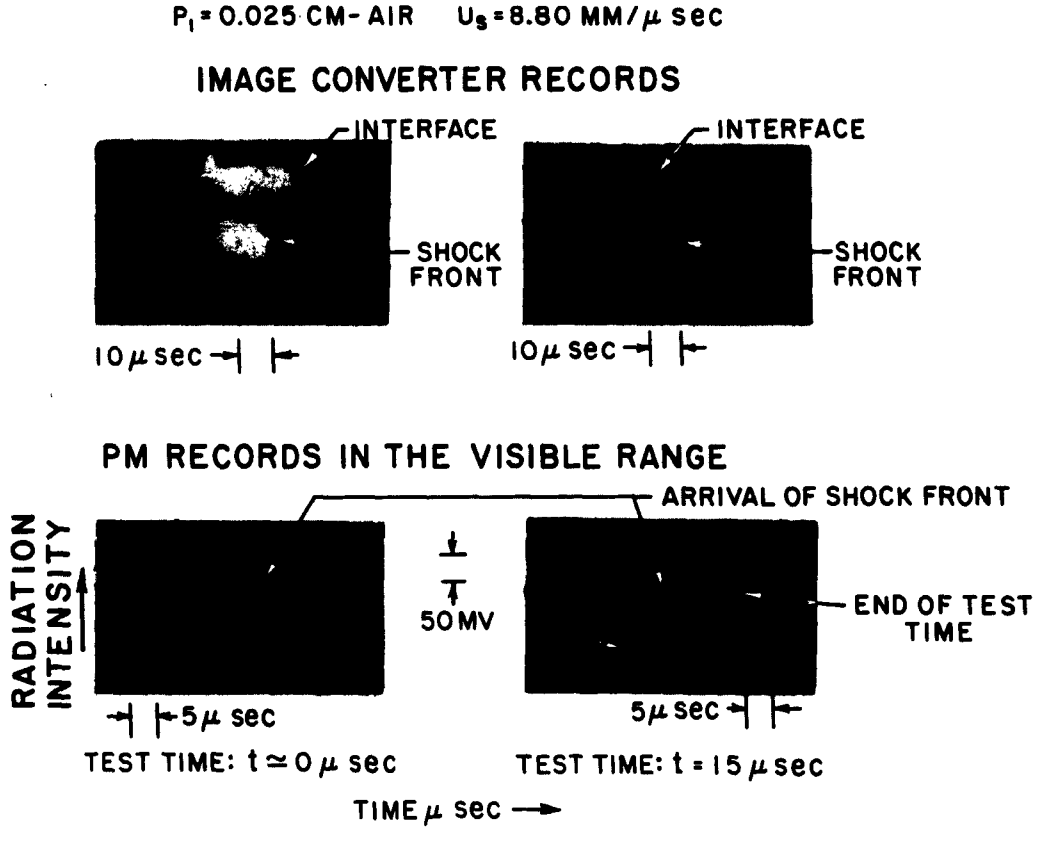

Fig. 9 Instantaneous photographs of the shock-heated air and driver gas taken with an image converter (STL Model C). There are three .05 μsec exposures in each picture taken at 10μsec intervals. Right hand picture shows a properly developed hot gas test slug followed by a turbulent interface. Left hand picture shows the interface and shock front unresolved representative of a run during which no test gas has accumulated.

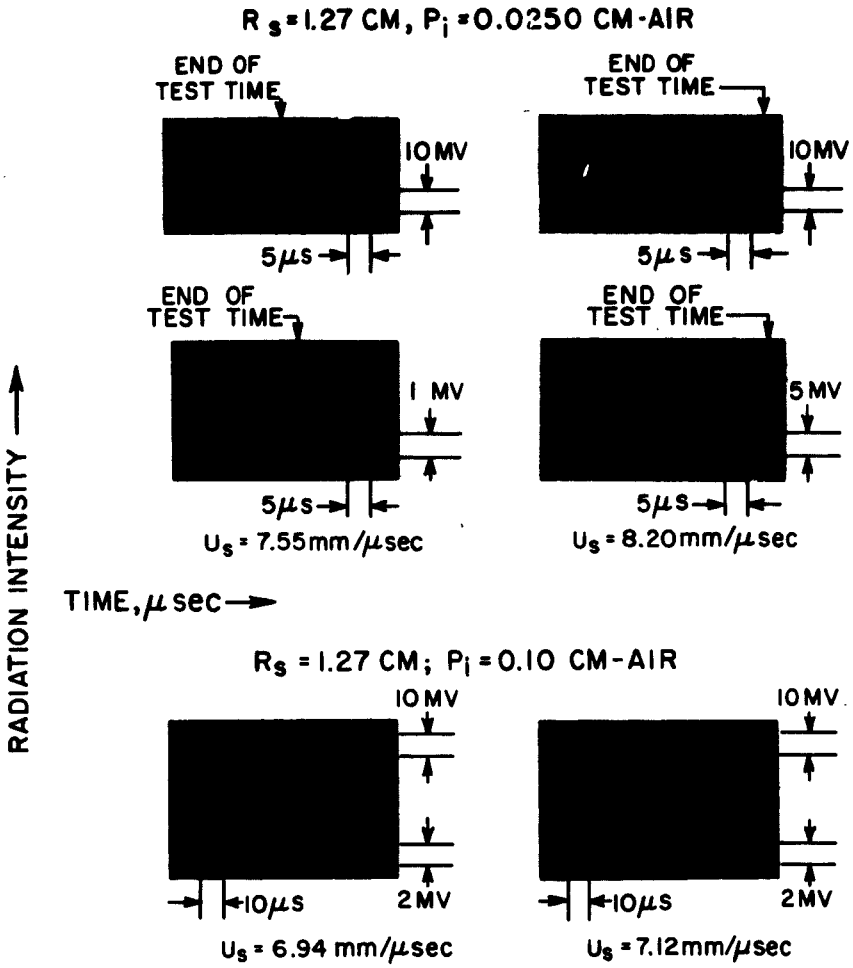

Fig. 10 Radiation emitted from the inviscid flow behind the bow shock of a heat transfer model. The photomultiplier viewed a vertical slit 1/2 mm wide, while the shock detachment distance was approximately 2 mm, and thus sees the gas in front of the stagnation point. The slight, fast initial rise is interpreted as the passage of the incident shock before it reaches the model. The slower rise to the equilibrium level is interpreted to be due to the time required by the flow geometry to establish its equilibrium configuration, see Fig. 6. The second rise corresponds to the arrival of the interface as also seen in the incident shock radiation, see Fig. 8.

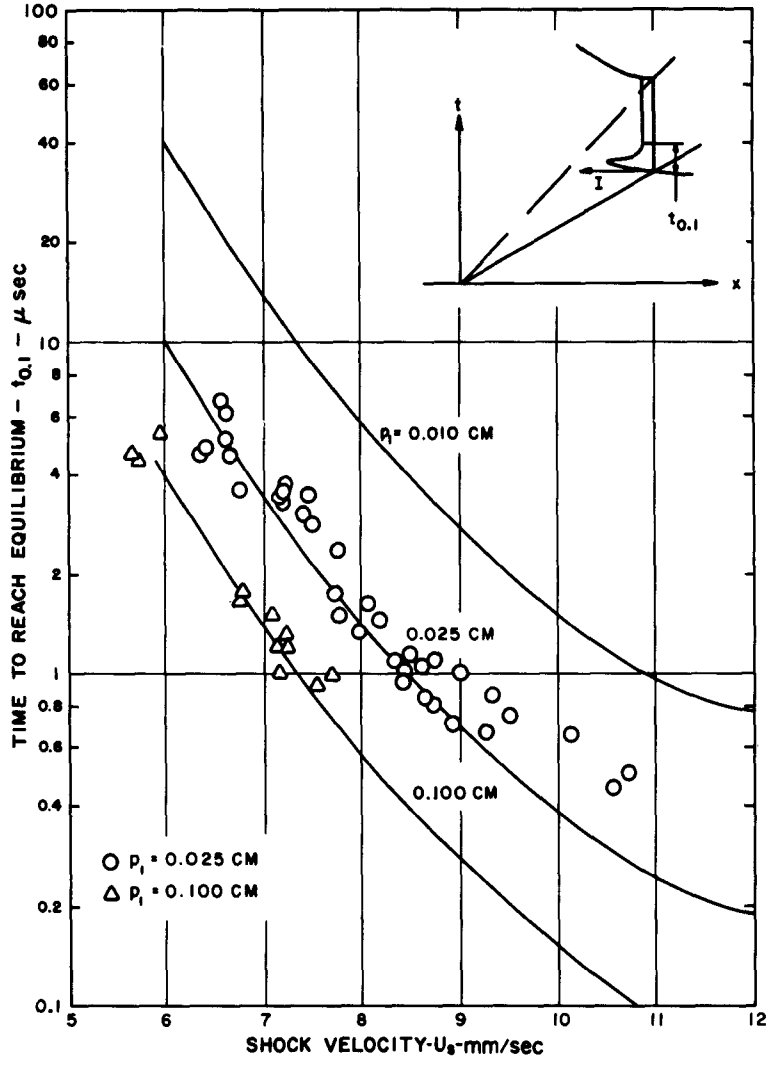

Fig. 11 Chemical equilibration time in air. Time or distance behind a normal shock at which the radiation from the nitrogen molecule band systems will decay to within 10% of the equilibrium value. Times were calculated from data of Ref. (18) and data points were observed in present experiments, i.e., Fig. 8. Limit of time resolution of present data is approximately 1/2 μsec.

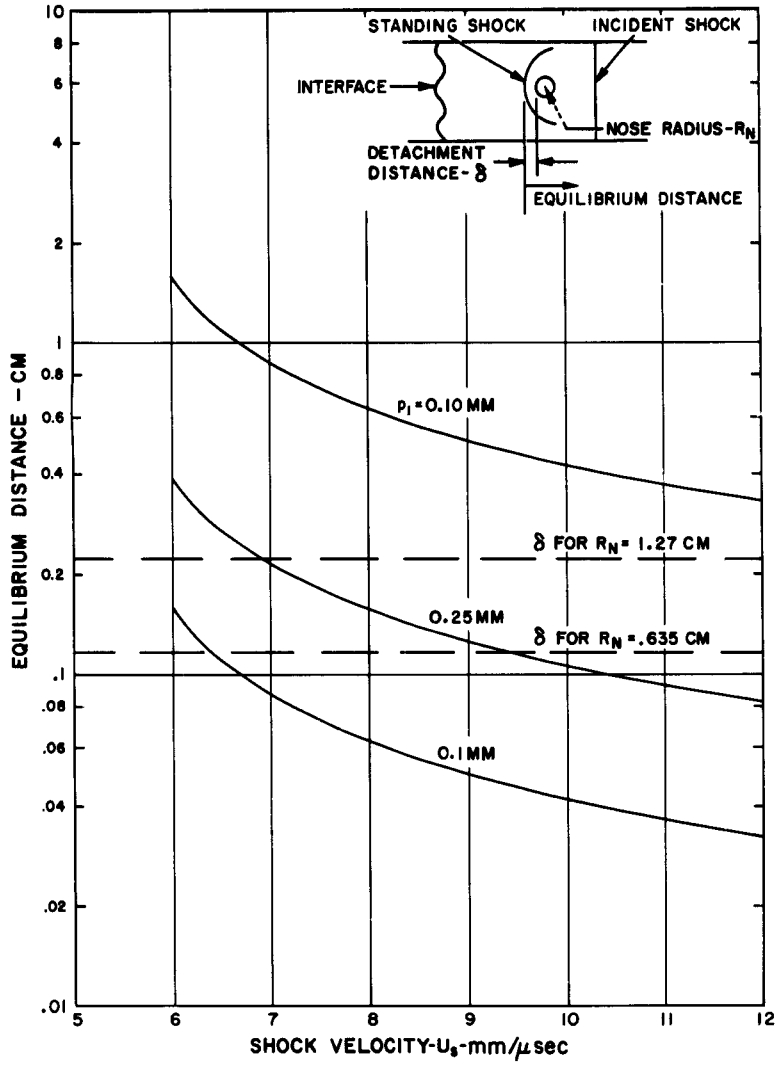

Fig. 12 Chemical equilibration distance behind standing shock. The distances shown were calculated by determining the particle time required to equilibrate air behind a normal shock in which the final conditions are the stagnation conditions shown. The data of Reference 17 and Fig. 11 were extrapolated to 50% higher velocities. This estimate is felt to be conservative because the gas ahead of the standing shock is already partially dissociated and equilibration from this condition should be faster than starting from cold gas.

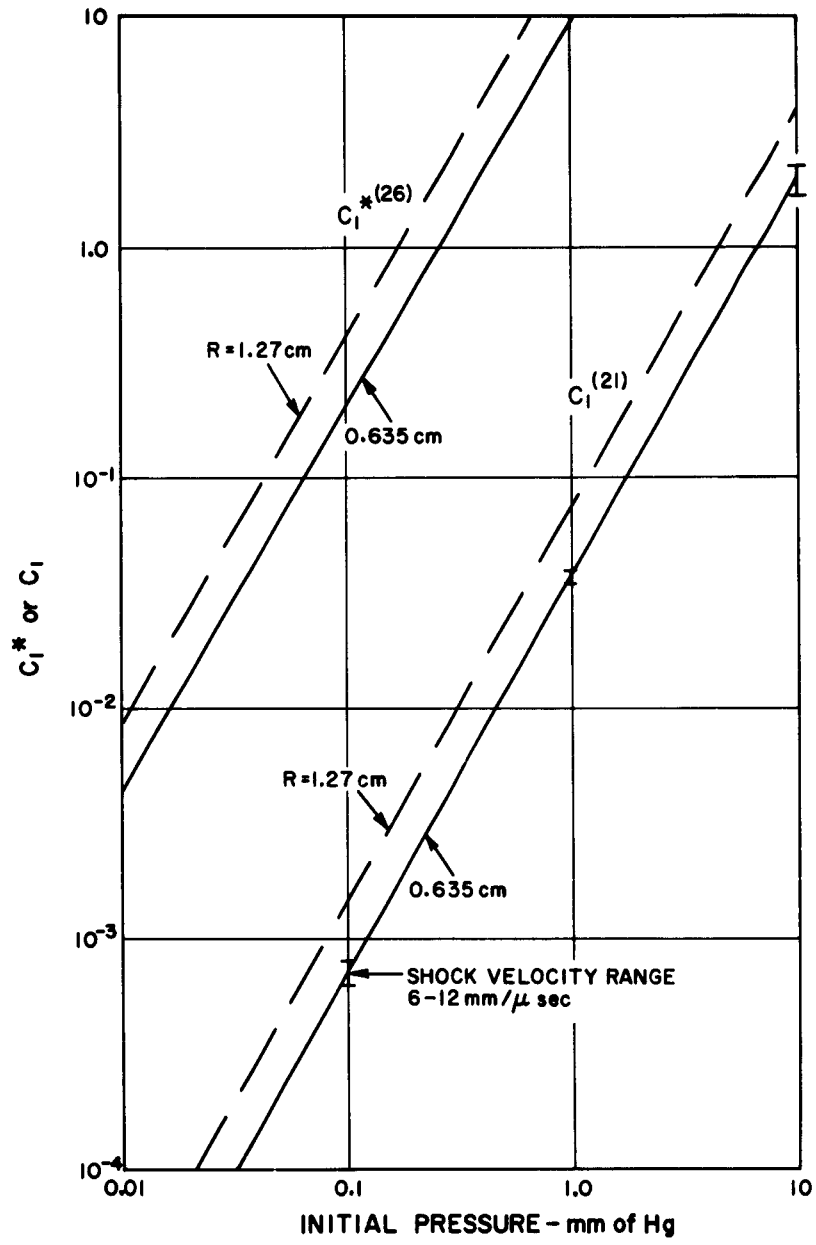

Fig. 13 State of dissociation equilibrium in the boundary layer. The parameters, C_1 and C_1^*, are the ratio of the recombination time for oxygen atoms to the diffusion time across the boundary layer, as defined in References 21 and 26, respectively.

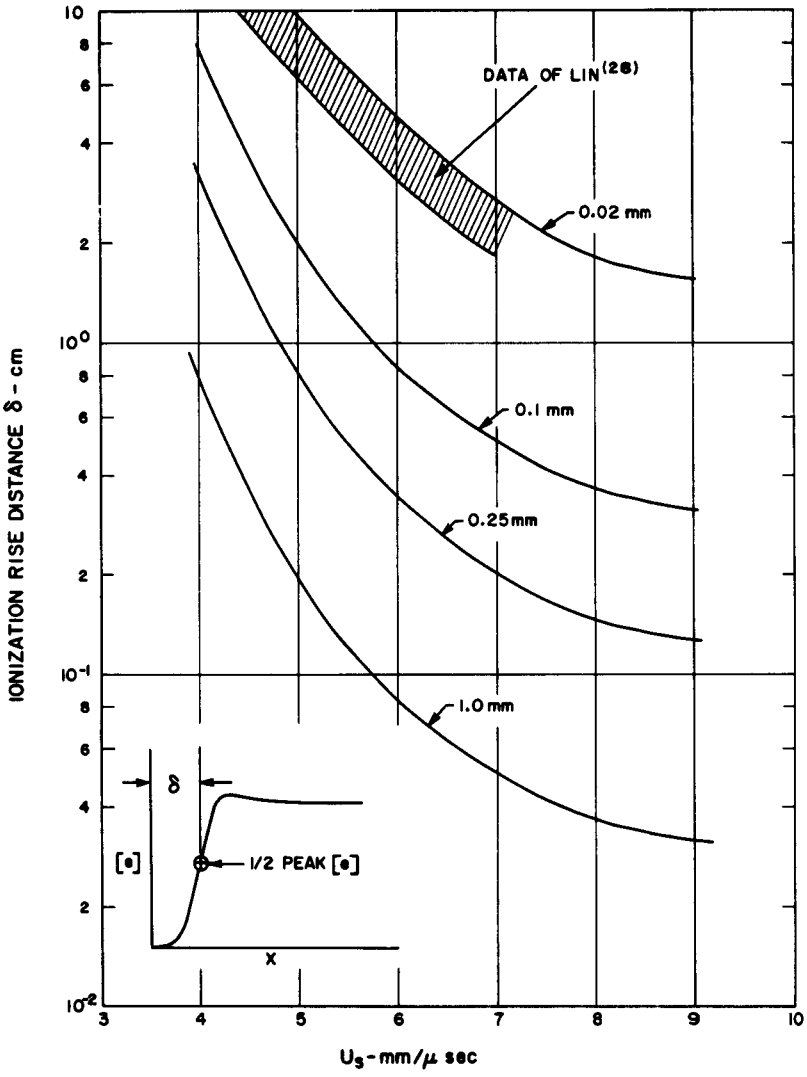

Fig. 14 Estimate of ionization distance or time behind a normal shock. Distance defined as the distance required to reach 50% of the peak electron concentration, from the data of Lin.[28] Region in which experiments were performed and agree with the theoretical model is shown. Other conditions are achieved by scaling the calculations.

A1019

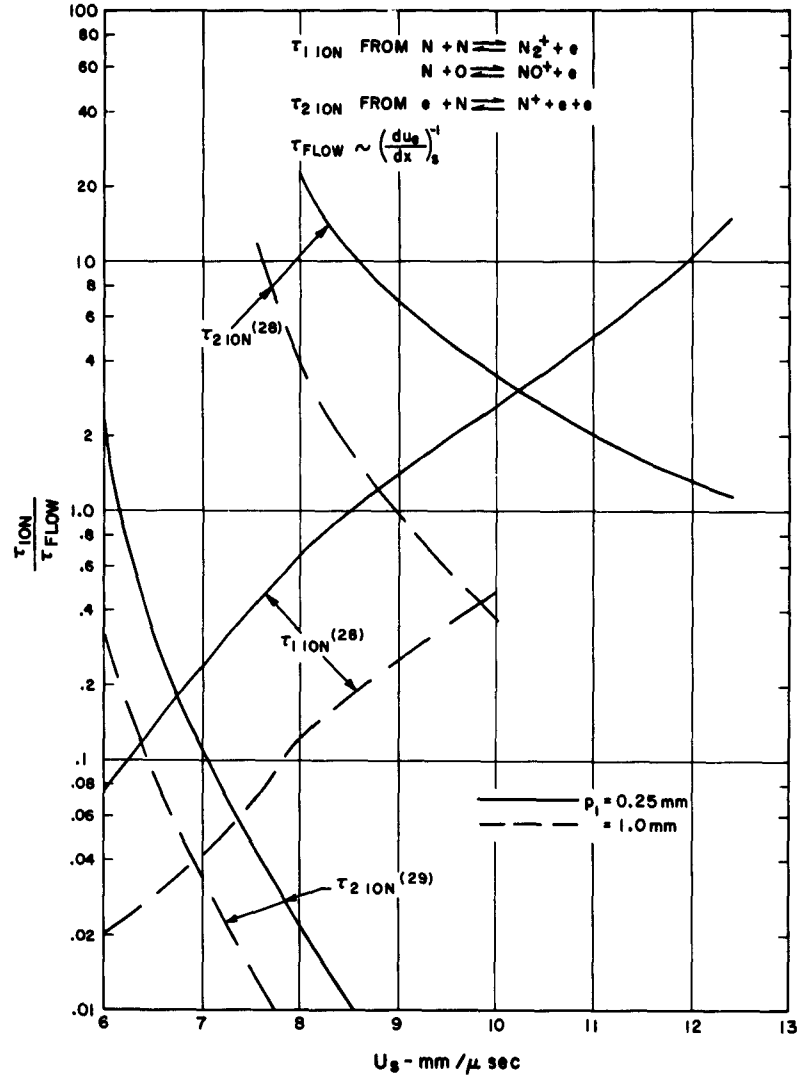

Fig. 15 Estimate of recombination of electrons in the boundary layer. τ_{1ion} for two-body recombination with molecular ions is slow at high shock velocity because of the small concentration of molecular ions. τ_{2ion} estimates from References (28) and (29) probably bracket the actual rates.

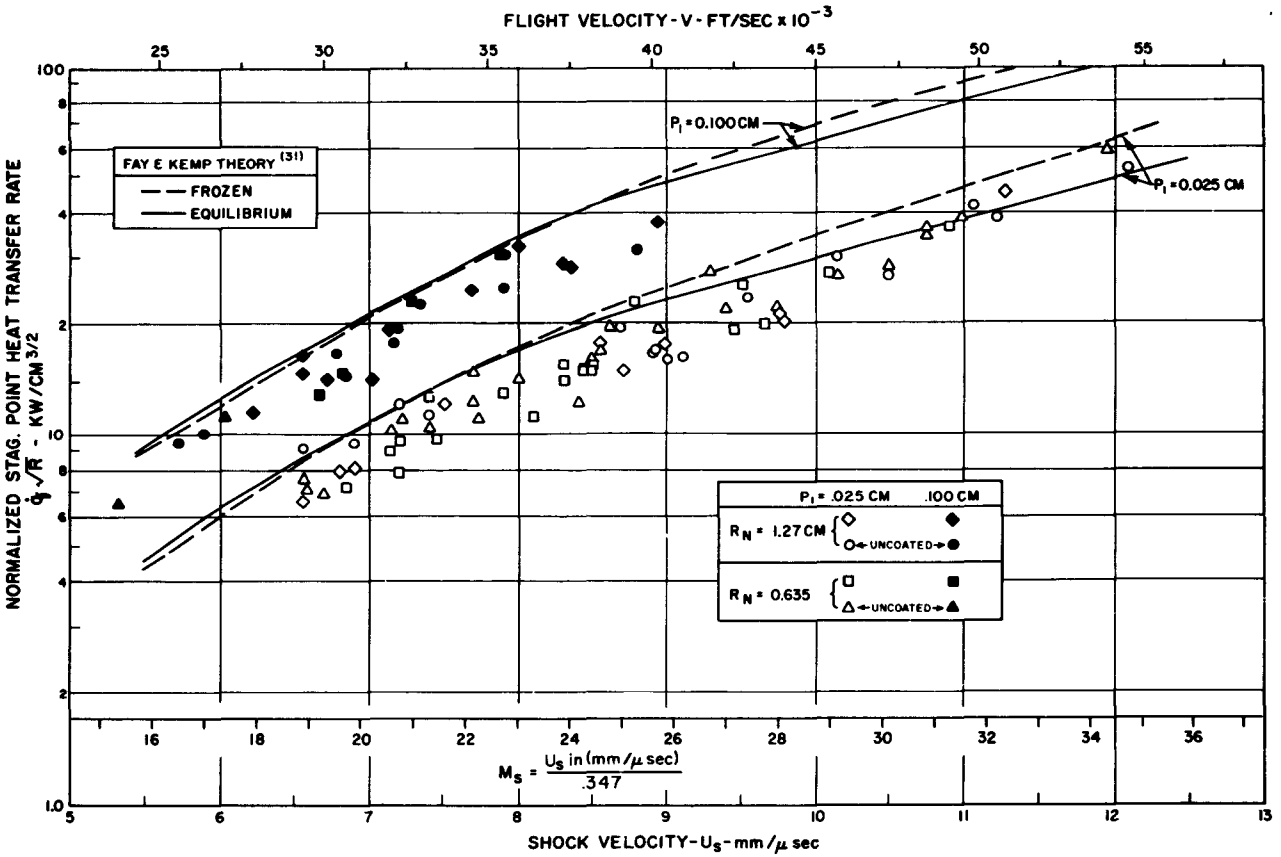

Fig. 16 Measured stagnation point heat transfer rates. Lines shown for comparison are the results of the calculations for the binary diffusion model for nitrogen at the appropriate conditions, from Fay and Kemp,[31] both for a frozen and equilibrium boundary layer.

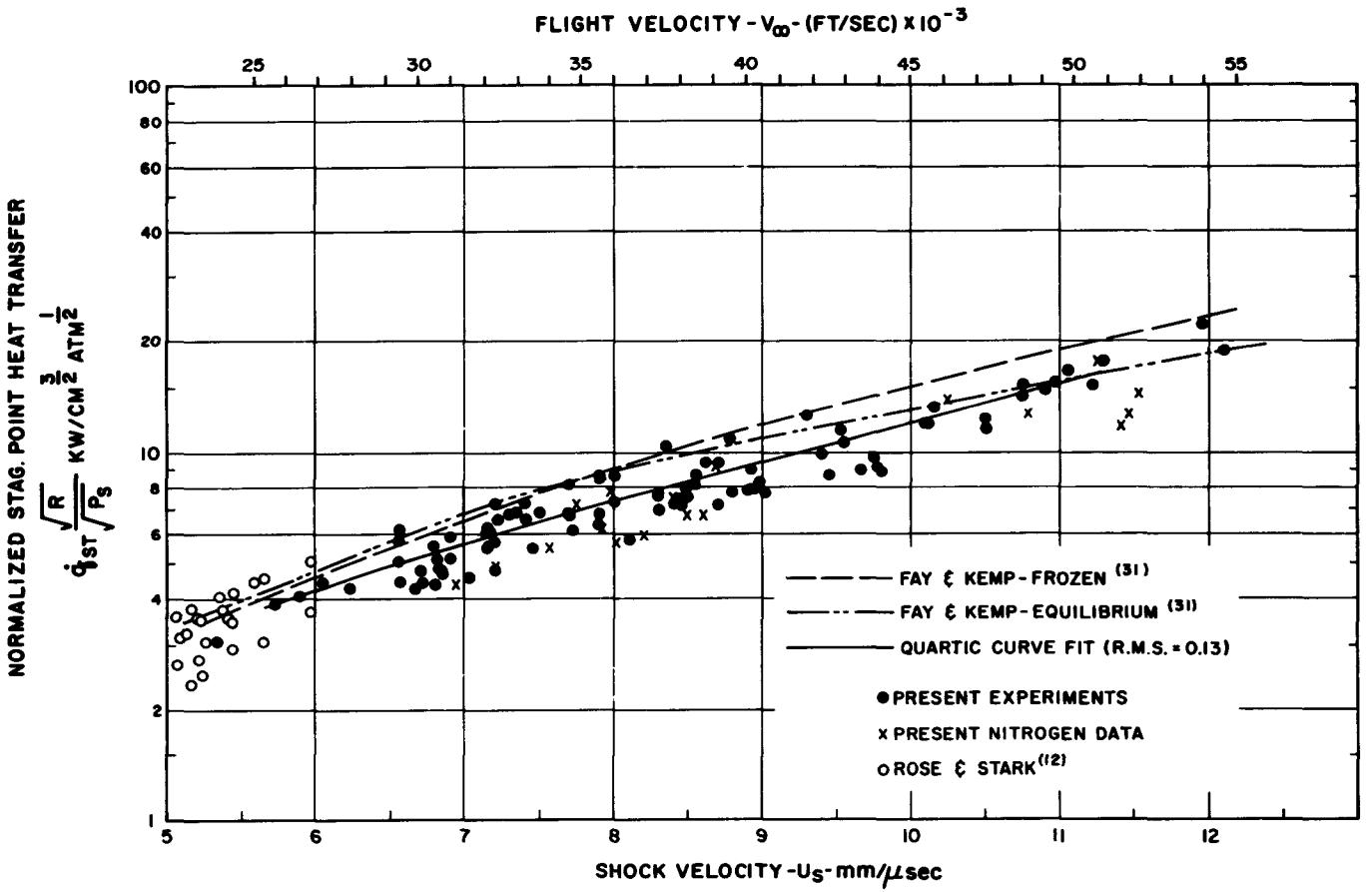

Fig. 17 Normalized stagnation point heat transfer results. Fay and Kemp results for an initial pressure of 0.25 mm of Hg are shown for comparison. A quartic curve fit to the data has RMS deviation of 0.13 and shows a maximum departure from the equilibrium theory of Ref. 31 of about 20% between shock velocities of 8 and 9 mm/μsec.

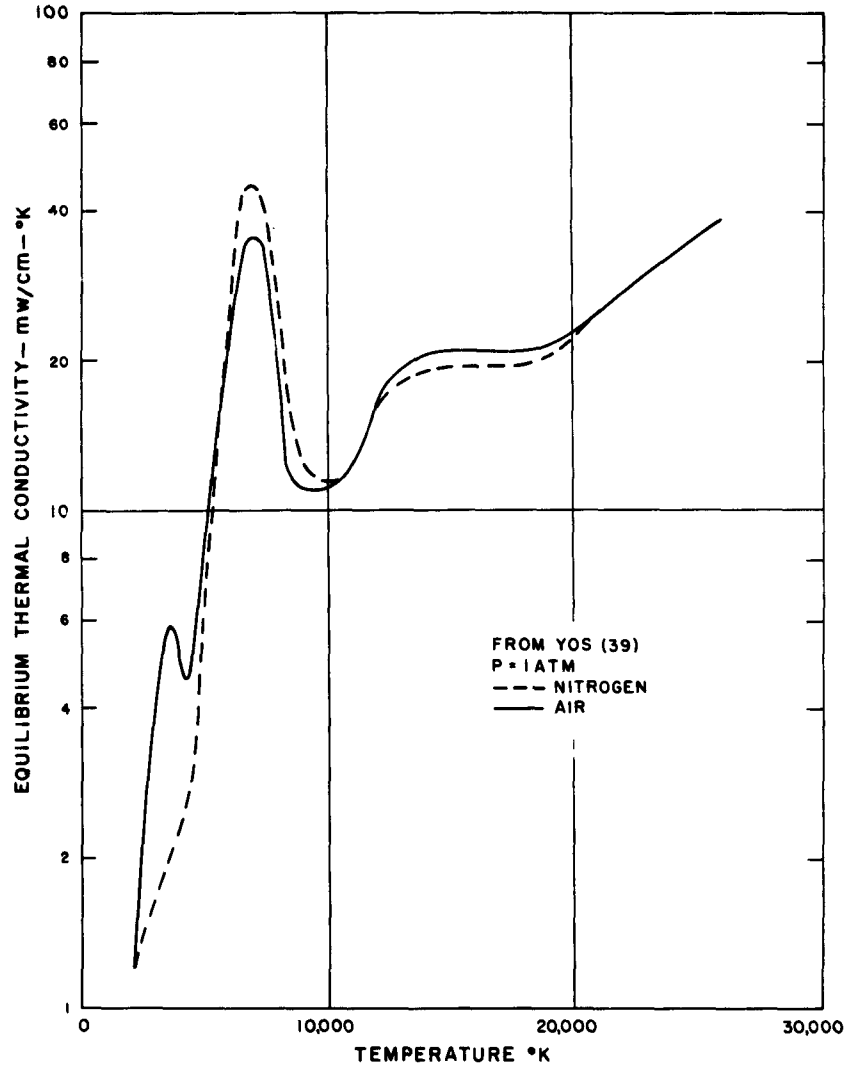

Fig. 18 Equilibrium thermal conductivity of air and nitrogen calculated by Yos.[39]

A1021

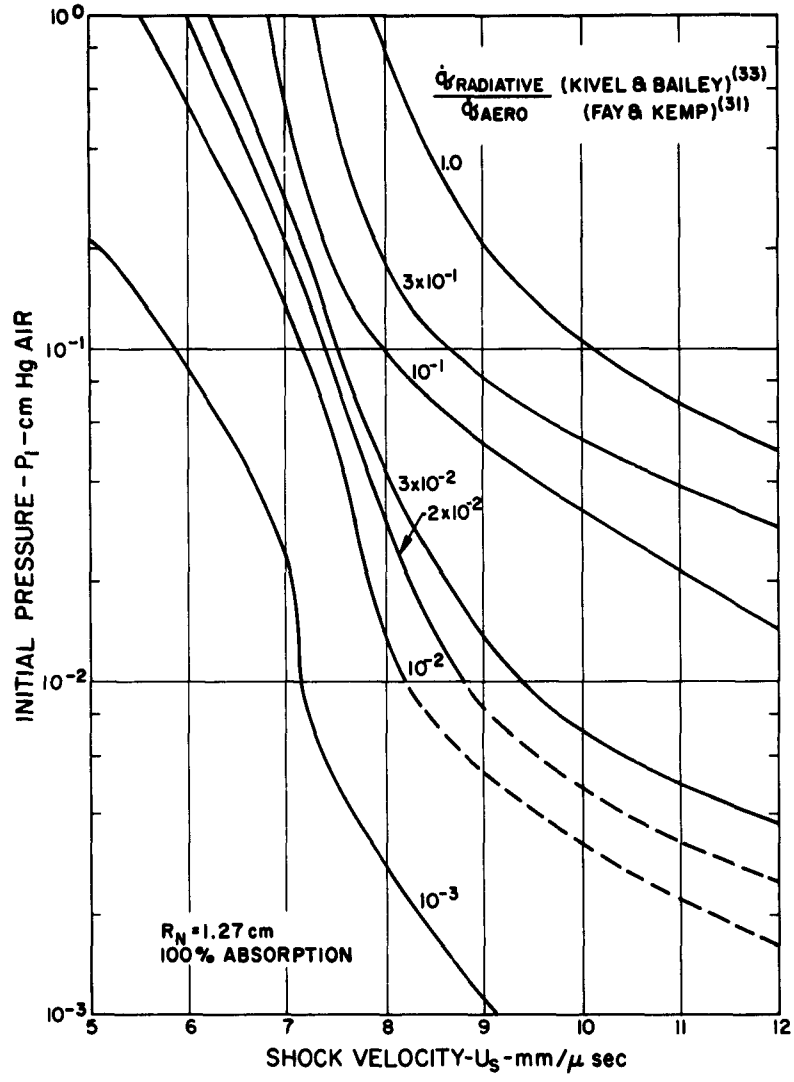

Fig. 19 Ratio of radiative and convective heating at the stagnation point of models used in the present experiments. Convective heating was calculated from Fay and Kemp,[31] equilibrium boundary layer and radiative heating was calculated from Kivel and Bailey,[33] assuming 100% absorption by the gage. Indications are that Reference (33) overestimates the radiation by approximately a factor of 2. The ratio scales as the nose radius to the three half power.

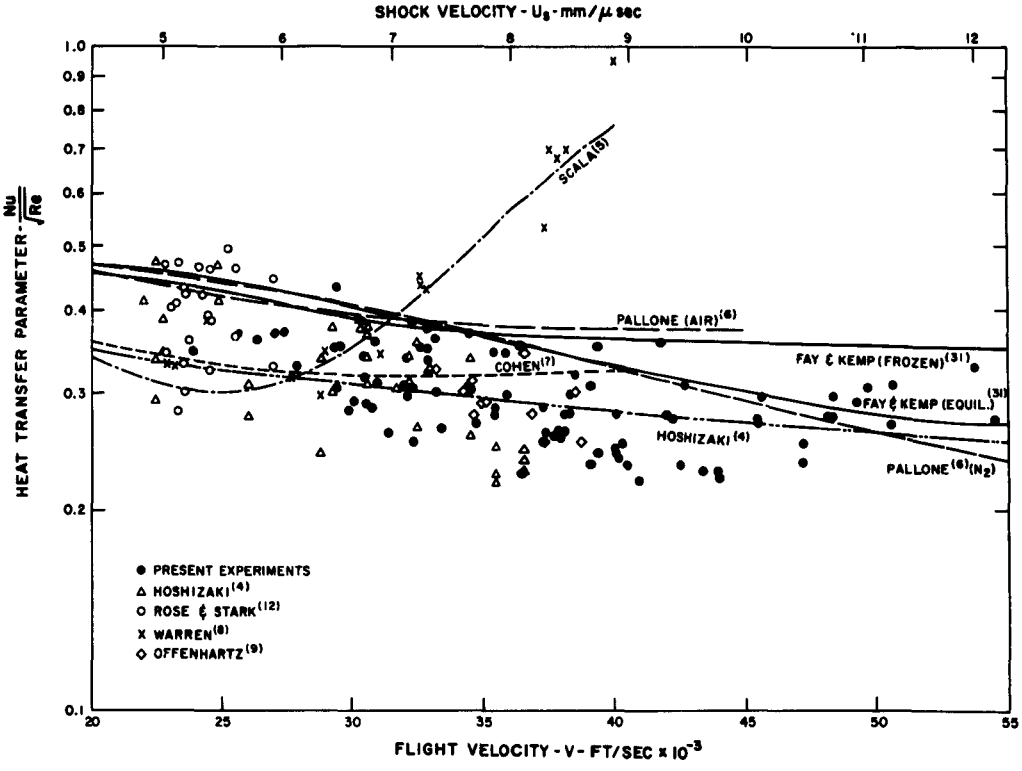

Fig. 20 Summary plot of various experimental data and theories for stagnation point heat transfer in partially ionized air and nitrogen. Pallone[6], Hoshizaki[4] and Cohen[7] theories are shown applicable to a stagnation pressure of 1 atm. Fay and Kemp[31] was calculated for the experimental conditions, i.e., p_1 = 0.25 mm of Hg. Scala[5] was calculated for a flight altitude of 240,000 ft.

REFERENCES

1. Adams, M. C., "A Look at the Heat Transfer Problem at Super-satellite Speeds," Avco-Everett Research Laboratory AMP 53, December, 1960. ARS Report 1556-60.

2. Bershader, D. and Rutowski, R. W., "Studies of an Argon Shock Layer Plasma," Fourth Biennial Gas Dynamics Symposium, ARS Preprint No. 1998-61, August, 1961.

3. Van Der Noorda, R. S. L., "Heat Transfer Measurements from Strongly Ionized Argon Produced by Sting Shock Waves," Cornell University Graduate School of Aeronautical Engineering, Thesis, February, 1957.

4. Hoshizaki, H., "Heat Transfer in Planetary Atmospheres at Super-satellite Speeds," ARS Journal, 32, October, 1962.

5. Scala, S. M. and Warren, W. R., "Hypervelocity Stagnation Point Heat Transfer," ARS Journal, 32, January, 1962.

6. Pallone, A. and Van Tassell, W., "The Effects of Ionization on Stagnation-Point Heat Transfer in Air and in Nitrogen," Avco Research and Advanced Development Division, Technical Memorandum RAD TM 62-75, September, 1962.

7. Cohen, N., "Boundary Layer Similar Solutions and Correlation Equations for Laminar Heat Transfer Distribution in Equilibrium Air at Velocities up to 41,100 Feet Per Second," NASA Technical Report R-118, 1961.

8. Warren, W. R., Rogers, D. A. and Harris, C. J., "The Development of an Electrically-Heated Shock-Driven Test Facility, " MSVD General Electric TIS Rept. R62SD37, April, 1962.

9. Offenhartz, E., Weisblatt, H. and Flagg, R. F., "Stagnation Point Heat Transfer Measurements at Super-Satellite Speeds," Jour. Royal Aeronautical Society, January, 1962.

10. Camm, J. C. and Rose, P. H., "Electric Shock Tube for High Velocity Simulation," Avco-Everett Research Laboratory Research Report 136, July, 1962. Also, Phys. of Fluids, May, 1963 (to be published).

11. Roshko, A., "On Flow Duration in Low-Pressure Shock Tubes," Phys. Fluids, 3, 835 (1960).

12. Rose, P.H. and Stark, W.I., "Stagnation Point Heat Transfer Measurements in Dissociated Air," Jour. of Aero/Space Sci., Vol. 25, No. 2, February, 1958.

13. Vidal, R.J., "Model Instrumentation Techniques for Heat Transfer and Force Measurements in a Hypersonic Shock Tunnel," CAL Rept. No. AD-917-A-1, WADC TN 56-315, February, 1956.

14. Rose, P.H., "Development of the Calorimeter Heat Transfer Gage for Use in Shock Tubes," Review of Scientific Instruments, Vol. 29:557, July, 1958.

15. Camac, M. and Feinberg, R., "High Speed Infrared Bolometer," Avco-Everett Research Laboratory Research Report 120, March, 1962. AFCRL 942, AFOSR 1564.

16. Hartunian, R.A. and Varwig, R.L., "A Correction to Thin-Film Heat Transfer Measurements," Aerospace Corp. Report, May, 1961.

17. Offenhartz, E. and Weisblatt, H., "Determination of the Time History of the Flow Field about Various Blunt Body Shapes and Sizes during Experiments in 1.5-inch Diameter Shock Tubes," Avco Research and Advanced Development Division Technical Report RAD TR-58-10, July, 1958.

18. Teare, J.D., Georgiev, S. and Allen, R.A., "Radiation from the Non-Equilibrium Shock Front," Progress in Astronautics and Rocketry, Vol. 7, Ed. by F.R. Riddell, New York. Academic, 1962.

19. Keck, J., Camm, J., Kivel, B. and Wentink, T., Jr., "Radiation from Hot Air, Part II," Annals of Physics, Vol 7:1, May, 1959.

20. Wray, K.L., "Chemical Kinetics of High Temperature Air," Avco-Everett Research Laboratory Research Report 104, June, 1961. Progress in Astronautics and Rocketry, Vol. 7, Ed. by F.R. Riddell, New York. Academic, 1962, also ARS Rept. 1975-61.

21. Fay, J.A. and Riddell, F.R., "Theory of Stagnation Point Heat Transfer in Dissociated Air," Jour. of Aero/Space Sci., Vol. 25, No. 2, February, 1958.

22. Britton, D., Davidson, N. and Schott, G., "Shock Waves in Chemical Kinetics," Faraday Society Discussion, 1954, No. 17.

23. Goodwin, G. and Chung, P.M., "Effects of Nonequilibrium Flows on Aerodynamic Heating During Entry into the Earth's Atmosphere from Parabolic Orbits," Advances in Aeronautical Sci., Vol. 4, September, 1960.

24. Wilson, J.A., "A Shock Tube Measurement of the Recombination Rate of Oxygen," Ph.D. Thesis, Cornell University, June, 1962.

25. Wray, K.L., "Shock Tube Study of the Recombination of O-Atoms by Ar Catalysts at High Temperatures," Avco-Everett Research Laboratory Research Report 142, September, 1962.

26. Inger, G.R., "Correlation of Surface Temperature Effect on Non-Equilibrium Heat Transfer," ARS Jour., 32, November, 1962.

27. Lin, S.C., and Fyfe, W.I., "Low-Density Shock Tube for Chemical Kinetic Studies," Phys. of Fluids, Vol. 4:238, Feb. 1961, also Avco-Everett Research Laboratory Research Rept. 91, July, 1960.

28. Lin, S.C. and Teare, J.D., "Rate of Ionization Behind Shock Waves in Air. II. Theoretical Interpretation," Avco-Everett Research Laboratory Research Report 115, to be published in Physics of Fluids.

29. Bates, D.R., "Atomic and Molecular Processes," Academic Press, 1962.

30. Hartunian, R.A., "Theory of a Probe for Measuring Local Atom Concentrations in Hypersonic Flows at Low Density," Aerospace Corp. Rept. No. TDR 930 (2230-06) TN-2, April, 1962.

31. Fay, J.A. and Kemp, N.H., "Theory of Stagnation Point Heat Transfer in a Partially Ionized Diatomic Gas," Avco-Everett Research Laboratory Research Report 144, December, 1962. Presented at IAS Annual Meeting, Jan. 1963, New York. IAS Preprint No. 63-60.

32. Fay, J.A., "Hypersonic Heat Transfer in the Air Laminar Boundary Layer," Avco-Everett Research Laboratory AMP 71, March, 1962. Presented at the Advisory Group for Aeronautical Research and Development Hypersonics Specialists' Conference, Brussels, Belgium, April 3-6, 1962.

33. Kivel, B. and Bailey, K., "Tables of Radiation from High Temperature Air," Avco-Everett Research Laboratory Research Report 21, December, 1957.

34. Breene, R. G., Jr., Nardone, M., Reithof, T. R. and Zeldin, S., "Radiance of Species in High Temperature Air," G. E. MSVD, TIS Report No. R62SD52, July, 1962.

35. Myerott, R. E., Sokoloff, J. and Nicholls, R. W., "Absorption Coefficients for Air," Geophysical Research Paper No. 58, GRD TN 60-277, July, 1960.

36. Keck, J. C. and Allen, R. A., "Transition Probabilities for Air Radiation," Presented at Symposium on Quantitative Spectroscopy at Elevated Temperatures and Selected Applications, California Institute of Technology, March 20-22, 1963.

37. Allen, R. A., Rose, P. H. and Camm, J. C., "Non-Equilibrium and Equilibrium Radiation at Supersatellite Re-Entry Velocities, IAS 31st Annual Meeting, New York, Jan. 1963. IAS Paper No. 63-77.

38. Hansen, C. F., "Approximations for the Thermodynamic and Transport Properties of High Temperature Air," NASA Technical Report R-50, NASA, Washington, D. C. (1959).

39. Yos, J. M., "Transport Properties of Nitrogen, Hydrogen, Oxygen and Air to 30,000°K," Research and Advanced Development Division, AVCO Corporation, RAD TM 63-7, January, 1963.

40. Scala, S. M., "Heating Problems of Entry into Planetary Atmospheres from Supercircular Orbiting Velocities," General Electric TIS Report No. R61SD176, October, 1961.

41. Private communication at NASA Headquarters, Washington, D. C., June 1, 1962.

42. Mason, E. A., Vanderslice, J. T. and Yos, J. M., "Transport Properties of High-Temperature Multicomponent Gas Mixtures," Phys. Fluids 2:688, (1959).

43. Maecker, H., "Experimental and Theoretical Studies of the Properties of N_2 and Air at High Temperatures," presented at the AGARD Meeting, Braunschweig, Germany, 1962.

44. Hacker, D. S. and Wilson, L. N., "Shock Tube Results for Hypersonic Stagnation Heating at Very Low Reynolds Numbers," Armour Research Foundation, Chicago, Illinois, ARF A-44.

45. Fenster, S. J. and Rozycki, R. C., Heat Transfer in a Partially Ionized Laminar Equilibrium Air Boundary Layer," Paper presented at 8th Midwestern Mechanics Conference, Cleveland, Ohio, April, 1963.

46. Fenster, S.J. and Heyman, R.J., "Heat Transfer in a Dissociated Gas with Variable Heat of Dissociation," Martin Company Report R 62-16 (1962).

47. Peng, T. and Pindroh, A.L., "An Improved Calculation of Gas Properties at High Temperatures: Air." Boeing Airplane Co. Document D2-11722 (1962).

Avco - Everett Research Laboratory, Everett, Massachusetts
STAGNATION POINT HEAT TRANSFER MEASUPEMENTS IN PARTIALLY IONIZED AIR, by P. H. Rose and J. O. Stankevics. April 1963. 49 p. incl. illus. (Avco - Everett Research Report 143; BSD - TDR - 62 - 348)
(Contract AF 04(694) - 33)

Unclassified report

Experimental measurements of convective stagnation point heat transfer in partially ionized air at simulated flight velocities up to 55,000 ft/sec are presented in this paper. Stagnation point heat transfer rates were measured in an arc - driven shock tube. The operation of this tube was carefully monitored by a variety of diagnostic techniques, mostly using emitted radiation as the observable. Although the performance of an arc - driven shock tube has been found to be quite predictable, it is shown that proper auxiliary measurements must be made for each experiment to identify those regions where proper flow conditions exist.

(over)

UNCLASSIFIED

1. Heat transfer.
2. Air, ionized - Heat transfer.
3. Re - entry physics.
4. Shock tubes.
I. Title.
II. Rose, P. H.
III. Stankevics, J. O.
IV. Avco - Everett Research Report 143.
V. AFBSD - TDR - 62 - 348.
VI. Contract AF 04(694) - 33.

UNCLASSIFIED

Avco - Everett Research Laboratory, Everett, Massachusetts
STAGNATION POINT HEAT TRANSFER MEASUREMENTS IN PARTIALLY IONIZED AIR, by P. H. Rose and J. O. Stankevics. April 1963. 49 p. incl. illus. (Avco - Everett Research Report 143; BSD - TDR - 62 - 348)
(Contract AF 04(694) - 33)

Unclassified report

Experimental measurements of convective stagnation point heat transfer in partially ionized air at simulated flight velocities up to 55,000 ft/sec are presented in this paper. Stagnation point heat transfer rates were measured in an arc - driven shock tube. The operation of this tube was carefully monitored by a variety of diagnostic techniques, mostly using emitted radiation as the observable. Although the performance of an arc - driven shock tube has been found to be quite predictable, it is shown that proper auxiliary measurements must be made for each experiment to identify those regions where proper flow conditions exist.

(over)

UNCLASSIFIED

1. Heat transfer.
2. Air, ionized - Heat transfer.
3. Re - entry physics.
4. Shock tubes.
I. Title.
II. Rose, P. H.
III. Stankevics, J. O.
IV. Avco - Everett Research Report 143.
V. AFBSD - TDR - 62 - 348.
VI. Contract AF 04(694) - 33

UNCLASSIFIED

Calorimetric heat transfer gages, either coated with silicon - monoxide films or uncoated, were used to measure heat transfer. The effects of boundary layer chemistry, radiation from the hot inviscid flow, and instrumentation errors are discussed. Comparison is made of the measured heat transfer rates with other data and the points of agreement and disagreement are analyzed. The data are compared to theoretical predictions made with a simple binary diffusion model of partially ionized diatomic gas, namely, nitrogen, whose transport properties were estimated from measured and calculated cross-section data. Stagnation point heat transfer rates calculated from this model for both a frozen and an equilibrium boundary layer, as well as equilibrium boundary layer results from other available calculations using more elaborate models of air, are compared to the data. The applicability of frozen and equilibrium calculations are discussed. Although it is not possible to differentiate between a number of the very similar theoretical treatments of this problem from the present results, it is concluded that the transport properties of air up to 15,000 ° K are known to reasonable accuracy and that heat conduction by electrons does not present a serious engineering problem for flight velocities up to 50,000 ft/sec.

UNCLASSIFIED

Calorimetric heat transfer gages, either coated with silicon - monoxide films or uncoated, were used to measure heat transfer. The effects of boundary layer chemistry, radiation from the hot inviscid flow, and instrumentation errors are discussed. Comparison is made of the measured heat transfer rates with other data and the points of agreement and disagreement are analyzed. The data are compared to theoretical predictions made with a simple binary diffusion model of partially ionized diatomic gas, namely, nitrogen, whose transport properties were estimated from measured and calculated cross-section data. Stagnation point heat transfer rates calculated from this model for both a frozen and an equilibrium boundary layer, as well as equilibrium boundary layer results from other available calculations using more elaborate models of air, are compared to the data. The applicability of frozen and equilibrium calculations are discussed. Although it is not possible to differentiate between a number of the very similar theoretical treatments of this problem from the present results, it is concluded that the transport properties of air up to 15,000 ° K are known to reasonable accuracy and that heat conduction by electrons does not present a serious engineering problem for flight velocities up to 50,000 ft/sec.

UNCLASSIFIED